



CATHODE MATERIALS FOR NEXT GENERATION LITHIUM-ION BATTERIES: DIAGNOSTIC TESTING AND EVALUATION OF LOW-COBALT CATHODES

Project ID: BAT252

DANIEL ABRAHAM

Argonne National Laboratory
June 1-4, 2020

2020 DOE Vehicle Technologies Office Annual
Merit Review

Overview

Timeline

- Start: October 1, 2018
- End: Sept. 30, 2021
- Percent complete: 50%

Budget

- Total project funding:
FY19 \$4.0M
- ANL, NREL, ORNL, LBNL, PNNL

Barriers

- Development of PHEV and EV batteries that meet or exceed DOE and USABC goals
 - Cost
 - Performance
 - Safety
 - Cobalt content

Team Members

- ANL, NREL, ORNL, LBNL, PNNL

Students supported from:

- University of Illinois at Chicago
- University of Rochester
- Oregon State University

Relevance

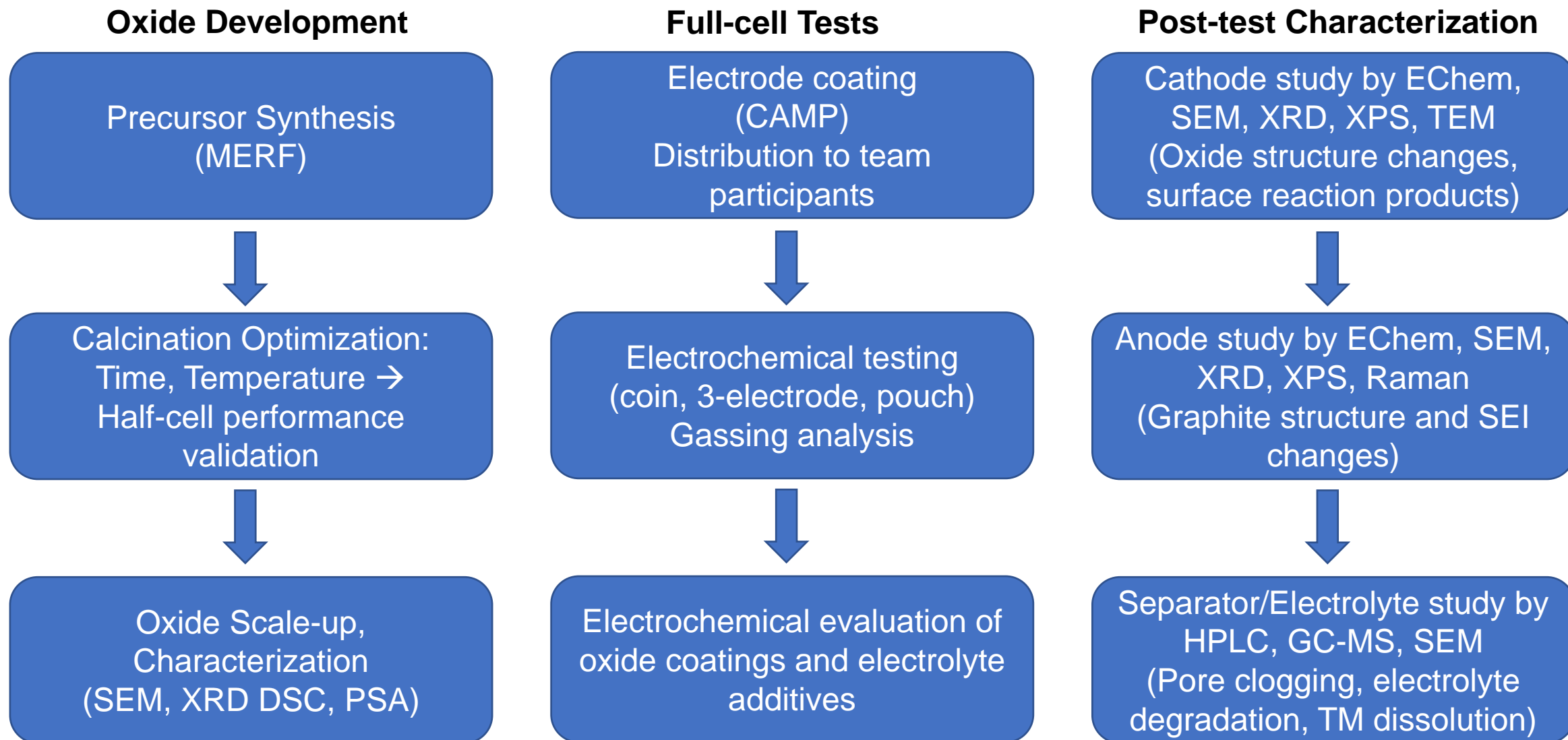
There is an urgent need to lower the cobalt content of transition-metal-based layered-oxides being considered for high-energy lithium-ion batteries in vehicular applications

- Lithiated layered oxides containing nickel, cobalt, and manganese, such as $\text{LiNi}_{0.6}\text{Mn}_{0.2}\text{Co}_{0.2}\text{O}_2$, are intercalation compounds used as positive electrodes in high-energy lithium-ion batteries
- To improve sustainability, lower cost, and minimize reliance on security critical materials, it is crucial to lower the cobalt content of these layered oxides
- Our main objective is to develop layered oxides with little or no cobalt, while maintaining the high energy densities, performance, and safety characteristics of the higher-cobalt oxides
- Another objective is to identify mechanisms associated with the performance loss (capacity fade, impedance rise) that occurs during extended cycling and to develop cell chemistries that provide a pathway to achieving cobalt-free cathodes

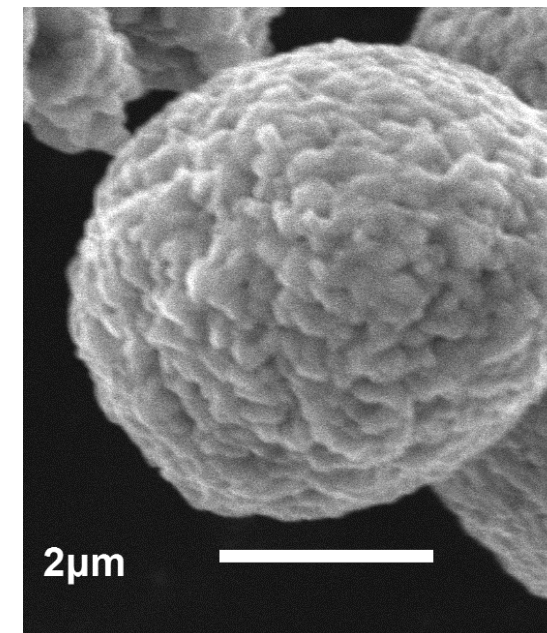
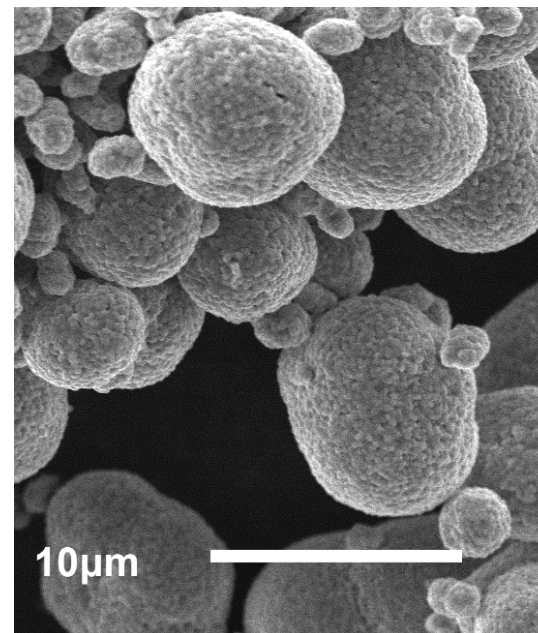
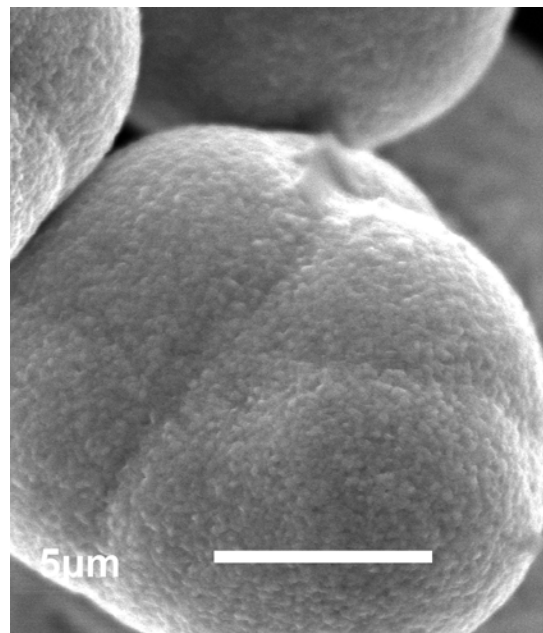
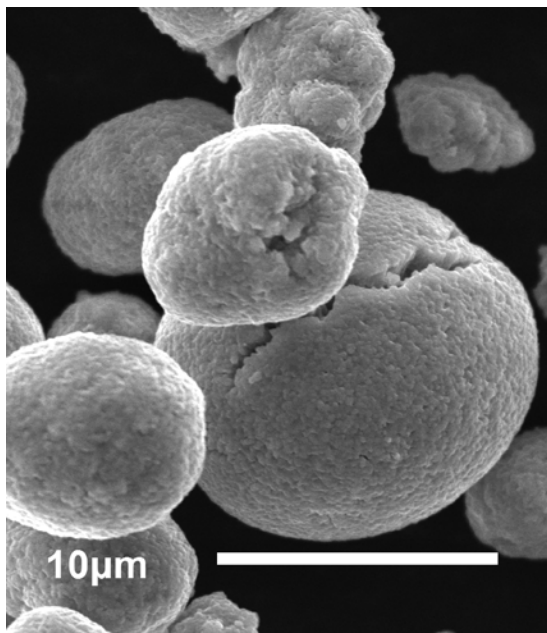
Approach

Also BAT251 & BAT253

Multi-institutional effort to identify and solve performance loss problems of full cells with low-Co layered-oxide cathodes



Electrodes fabricated at CAMP using oxides synthesized at MERF/CSE – SEM images from Post-test lab

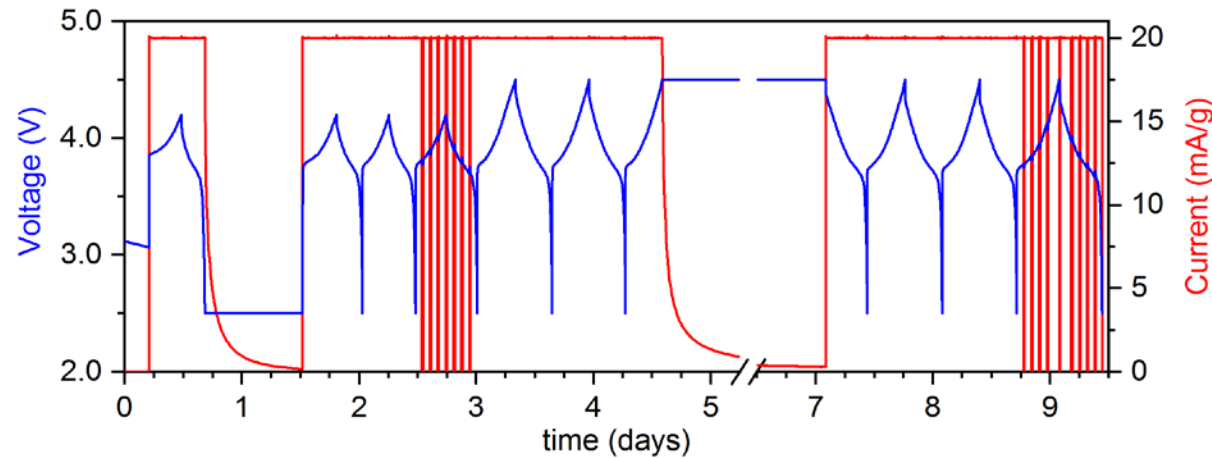


All cathodes contain 90 wt% oxide, 5 wt% carbons and 5 wt% PVdF binder.
Anodes contain 92 wt% graphite, 2 wt% carbons and 6 wt% PVdF binder.
Capacity-balanced electrodes: N/P ratio at 4.2 V cell voltage is $\sim 1.05 - 1.1$

See BAT 251, BAT167, BAT030

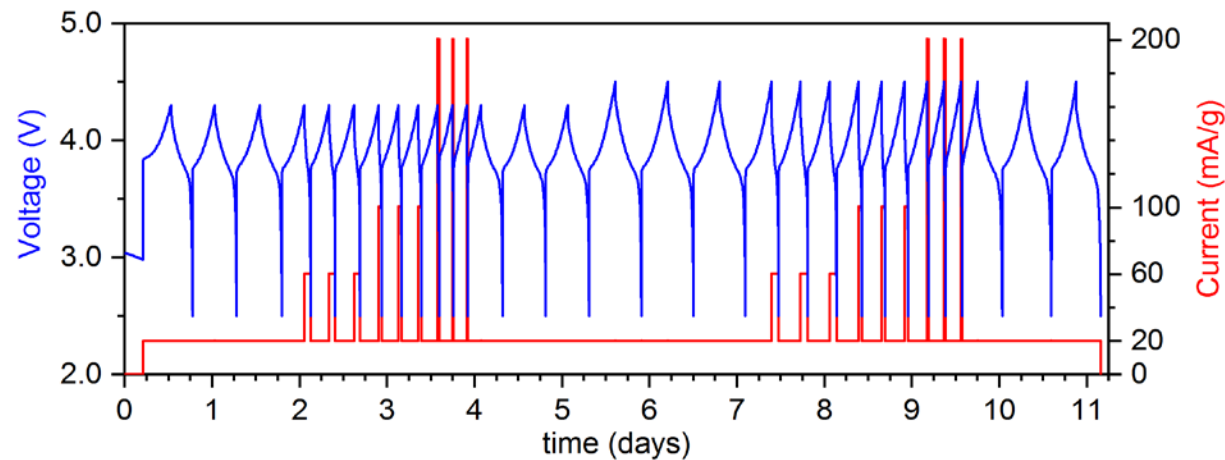
Half-cell (Li anode) tests on newly-synthesized oxides

Electrochemical test protocols developed to evaluate oxide properties and performance



Standard Protocol

Evaluates charge and discharge capacity, kinetic losses, and high voltage instability/damage with 4.2 V and 4.5 V UCV



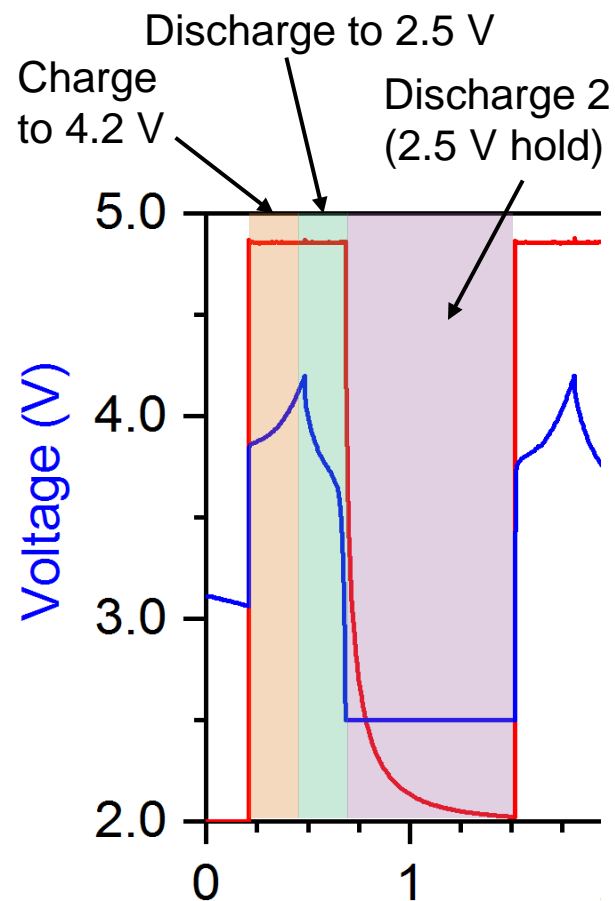
Rate Protocol

Evaluates discharge capacity at 4.3 V and 4.5 V UCVs with 20, 60, 100, 200 mA/g (charge is 20 mA/g), and damage due to cycling

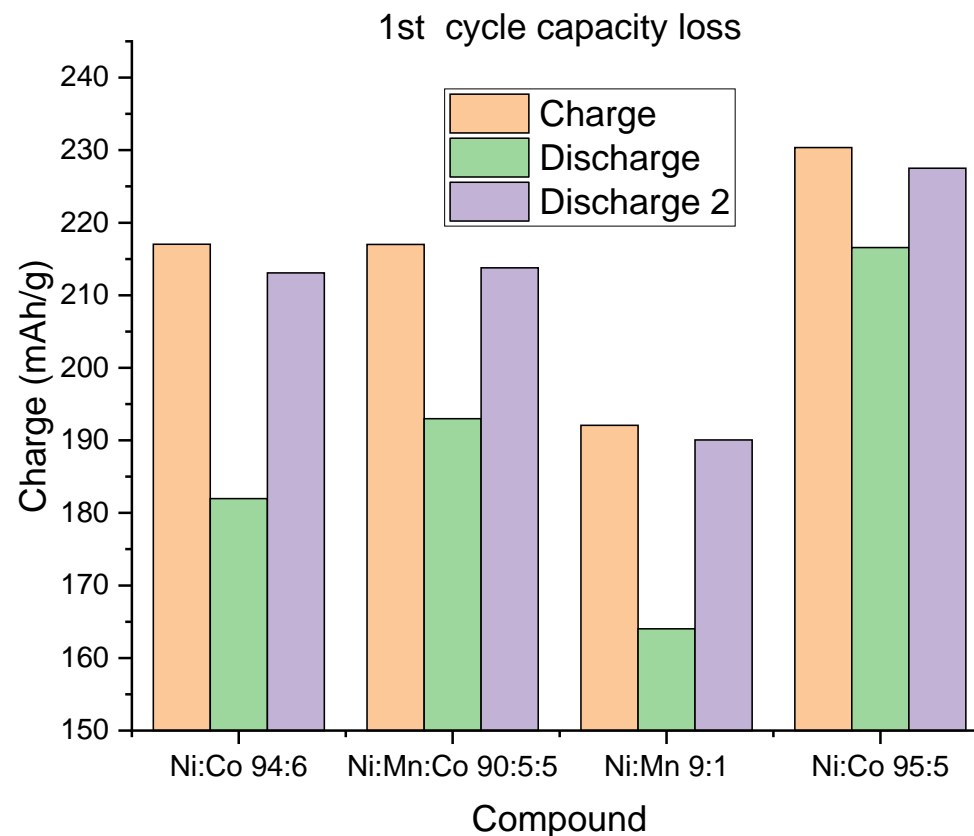
Test data help optimize synthesis conditions and validate electrochemical performance

Example data from standard protocol – 1st cycle metrics

Information on oxide capacities and kinetics limitations



Charge = Oxide delithiation
Discharge = Oxide lithiation
Discharge 2 provides information on kinetic limitations



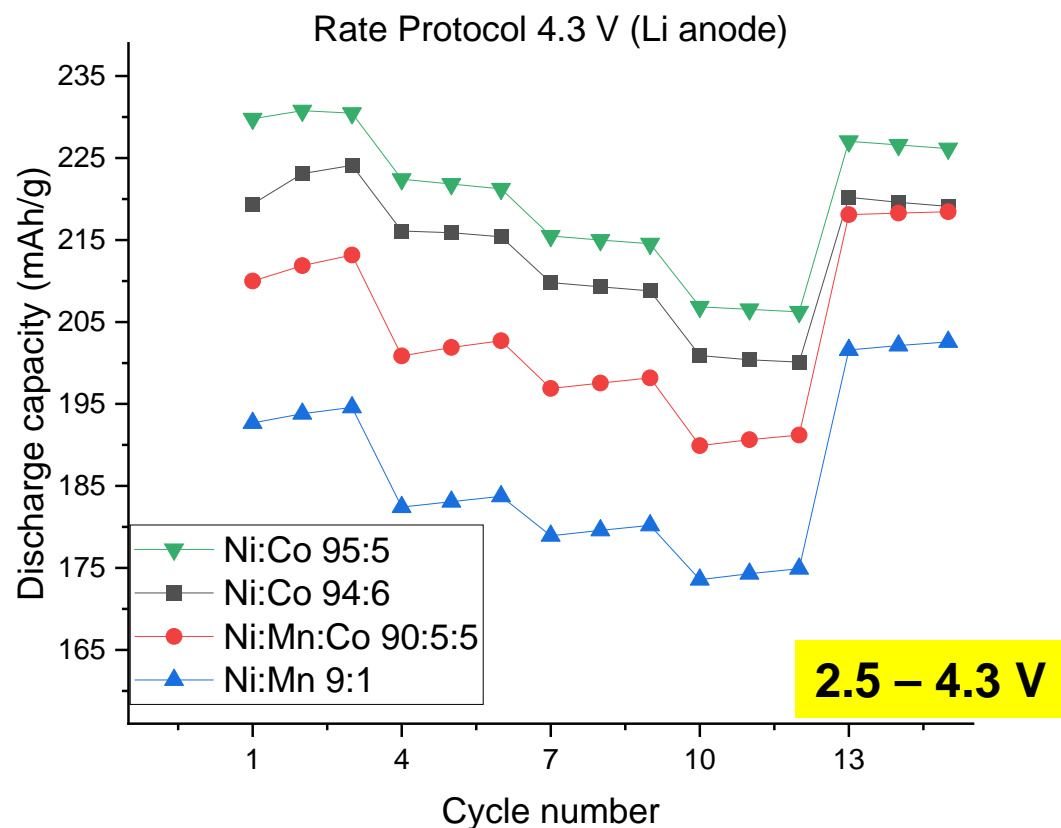
1st cycle “irreversible” capacity loss can be due to material degradation or electrode overpotentials

Equal values of ‘Charge’ and ‘Discharge 2’ indicate that 1st cycle losses are kinetic rather than due to oxide degradation

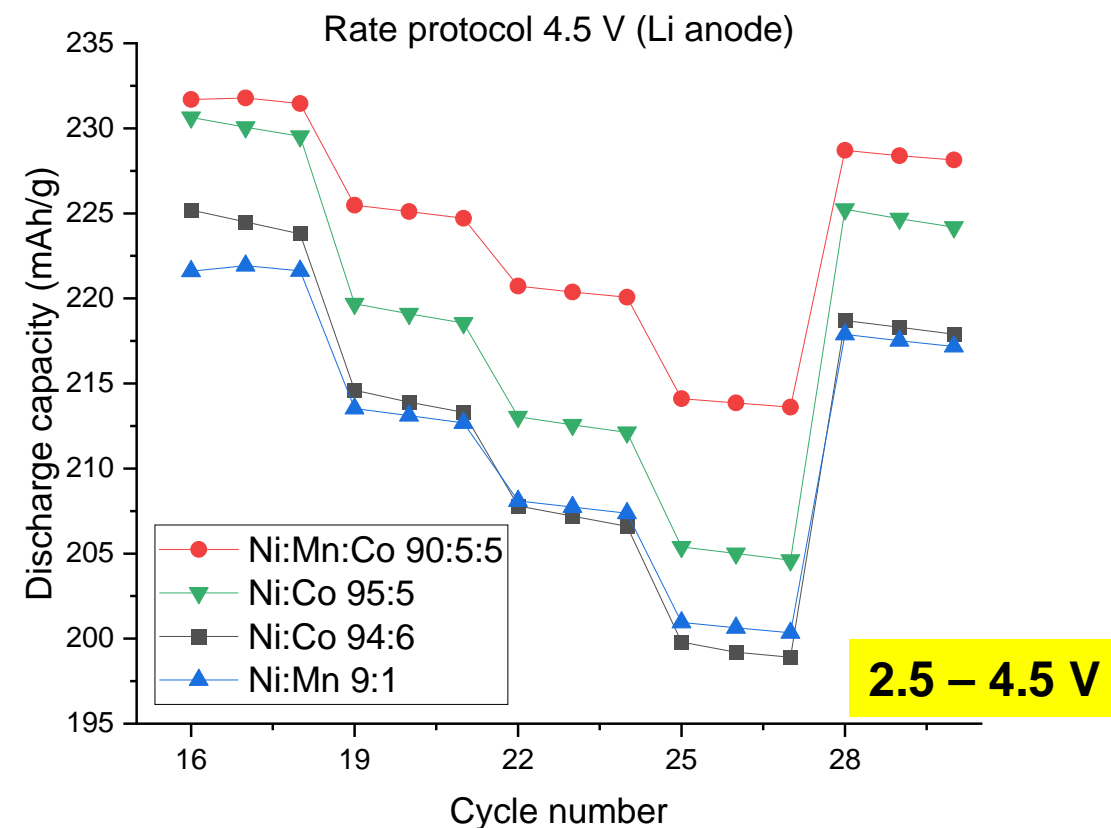
All oxides show minimal material degradation during the 1st cycle

Example data from rate protocol – capacity, stability

3 cycles each of 20 mA/g charge and 20, 60, 100, 200, and 20 mA/g discharge (15 cycles at 4.3 V and 4.5 V)



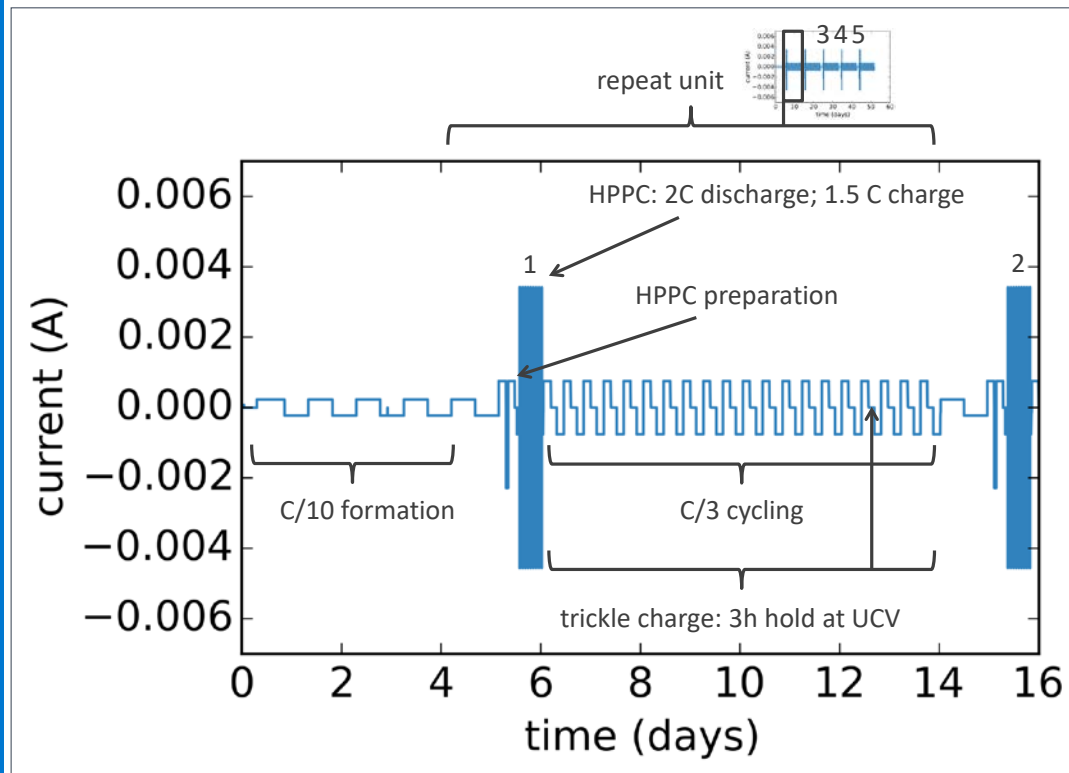
Larger differences between oxide capacities
Higher Ni oxides display higher capacities



Smaller differences between oxide capacities
Mn-containing oxides display higher stability

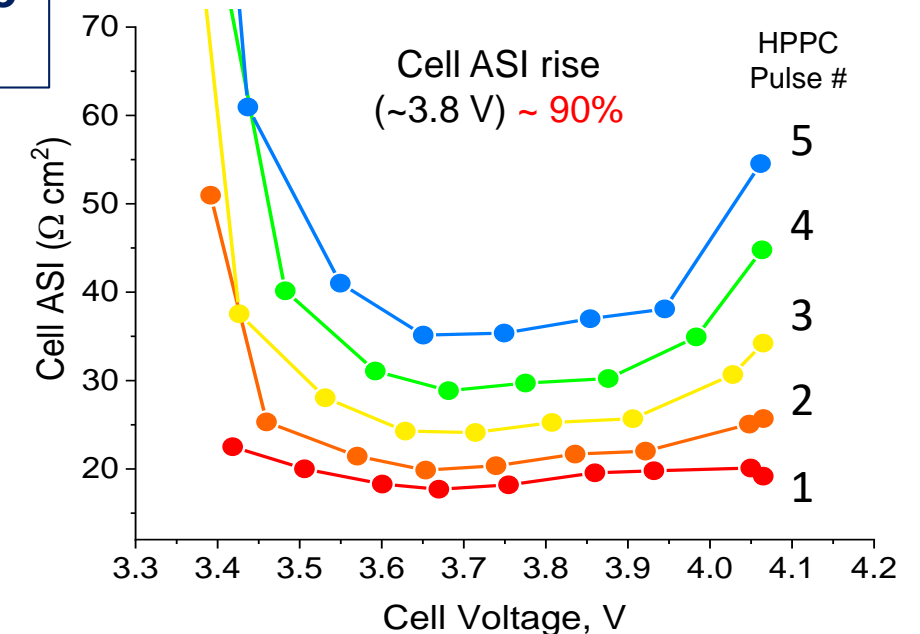
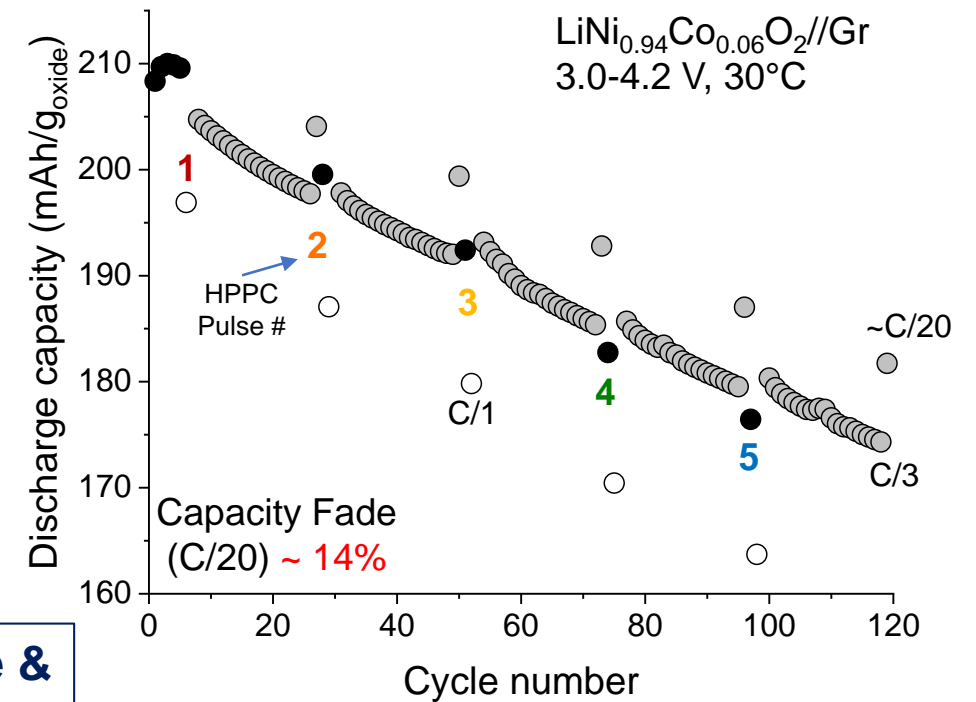
Standard cycling protocols used for full cell tests

Protocol includes 3h hold at 4.2 V to accelerate aging

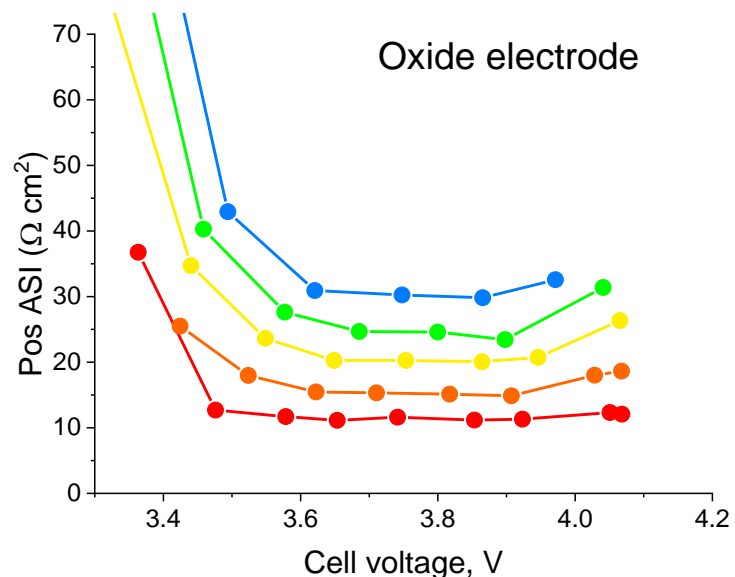
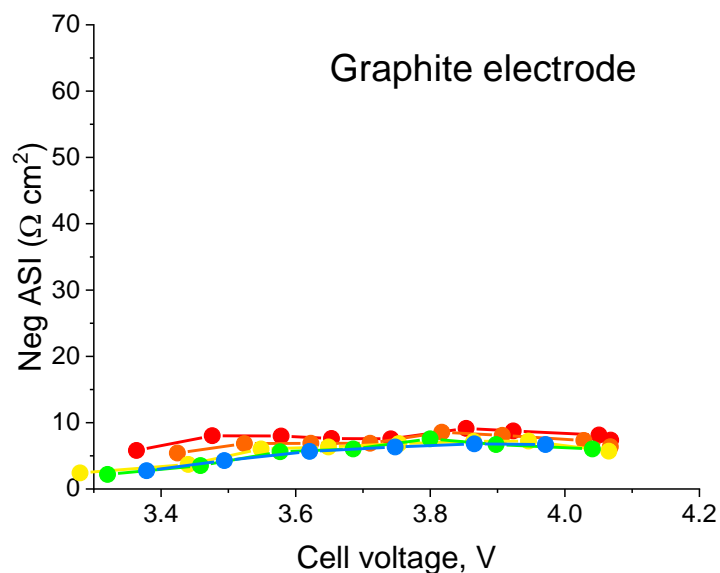
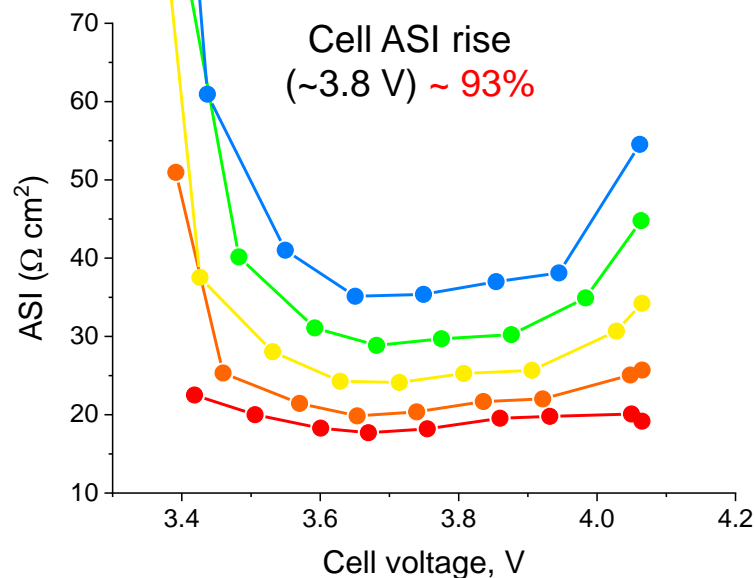
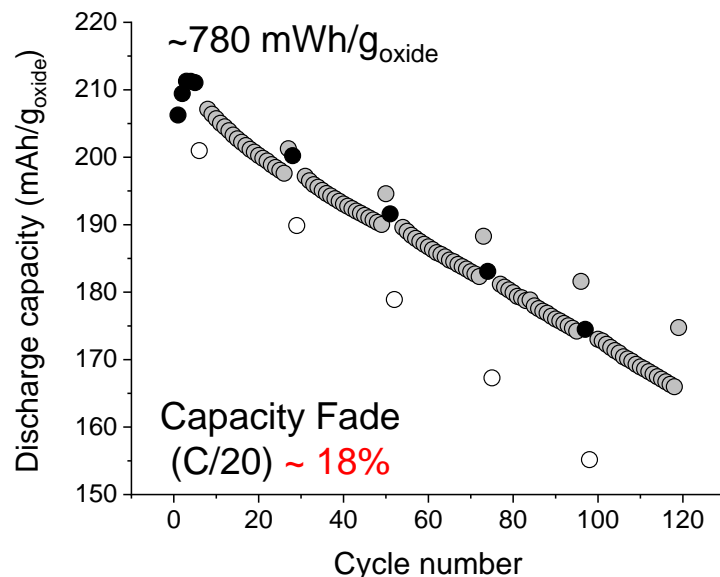


Capacity fade & Impedance rise during cycling

Protocol provides information on cell capacity and impedance changes

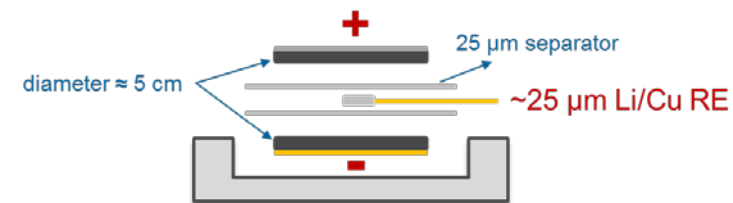


LiNi_{0.95}Co_{0.05}O₂//Gr cell: 3.0-4.2 V, 30°C, ~120 cycles



Coin Cell - typical data

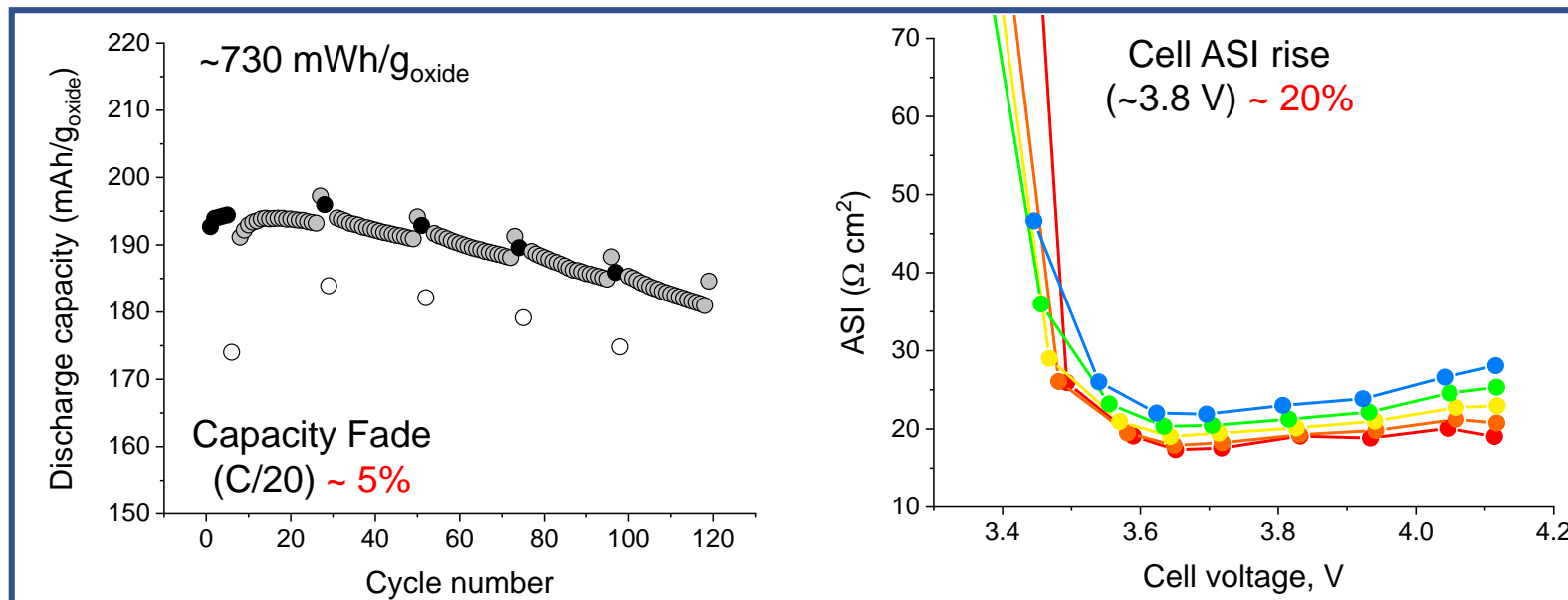
- Cell capacity and specific energy are excellent at the start but decreases on cycling
- Cell impedance progressively increases on cycling



3-electrode cell data

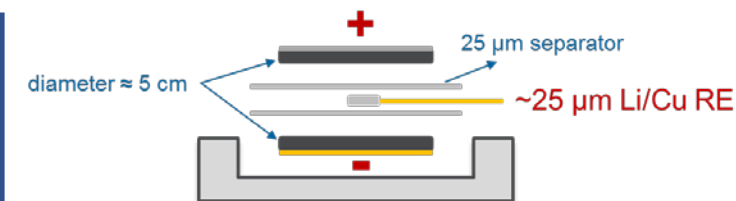
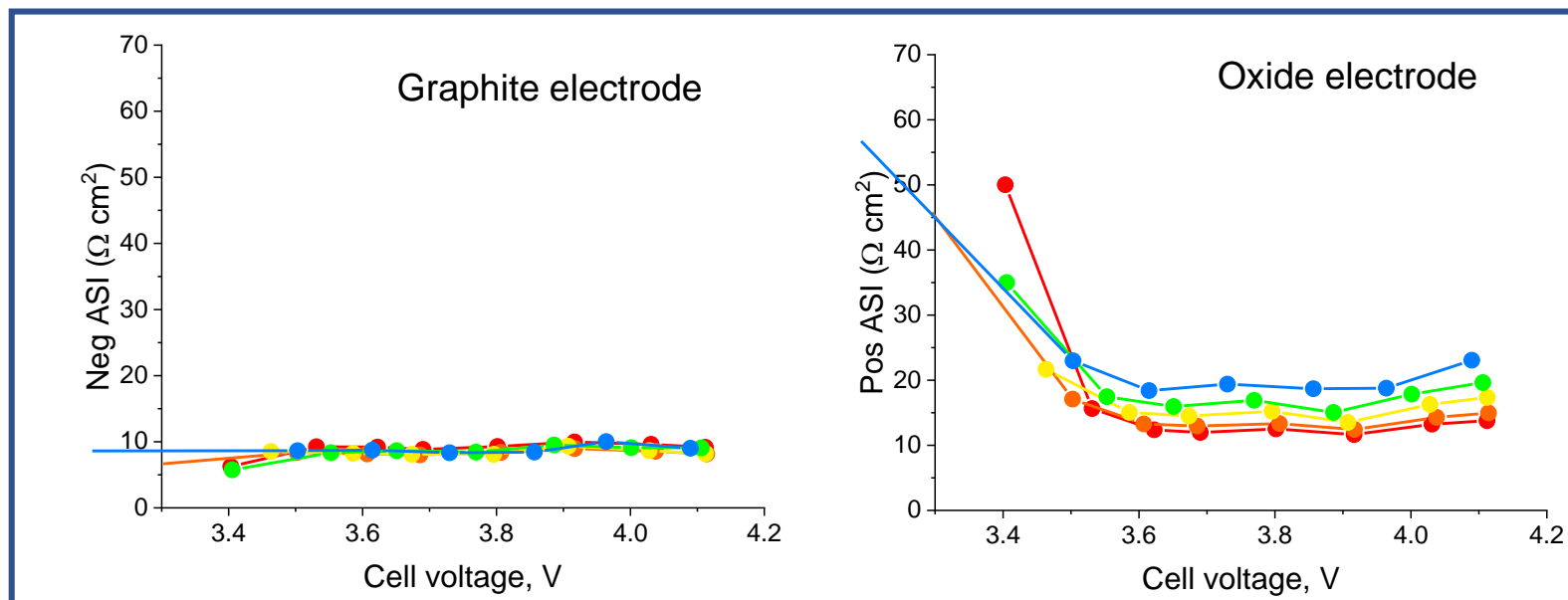
- Cell impedance increase arises at the positive electrode.
- Negligible ASI changes at the negative electrode

LiNi_{0.9}Mn_{0.1}O₂//Gr cell: 3.0-4.2 V, 30°C, ~120 cycles



Coin Cell - typical data

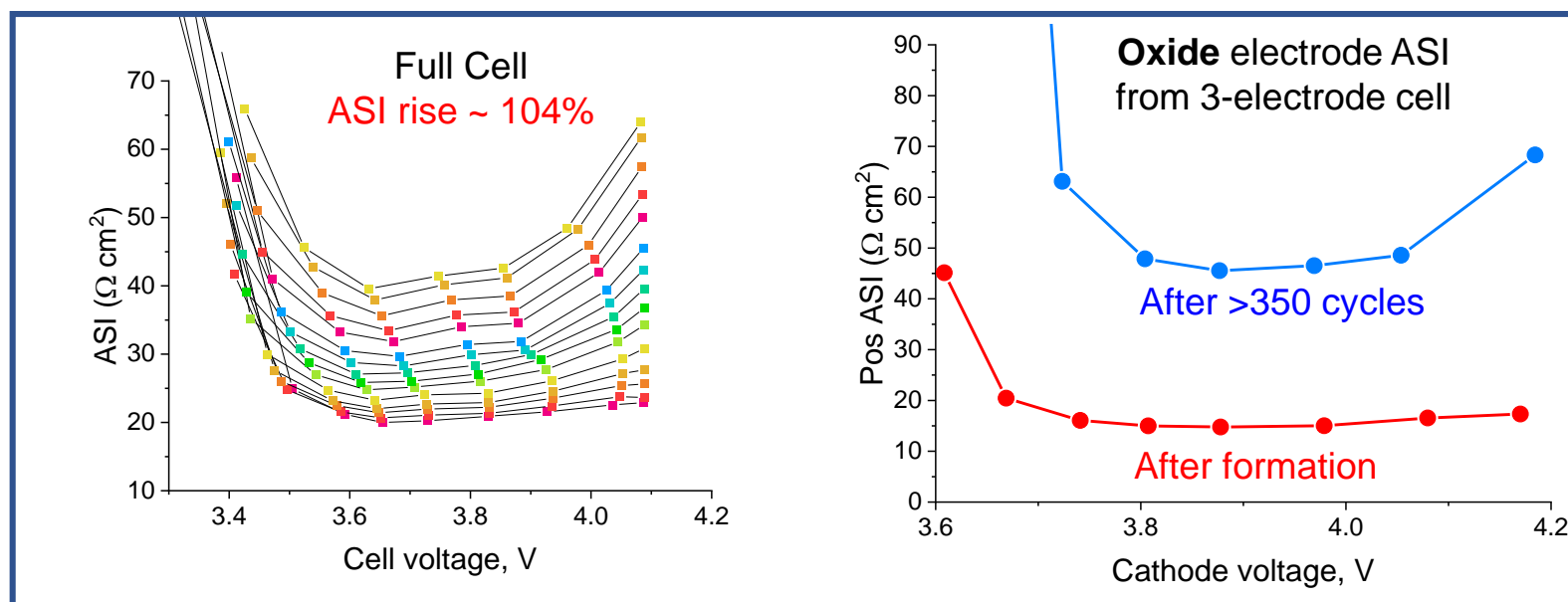
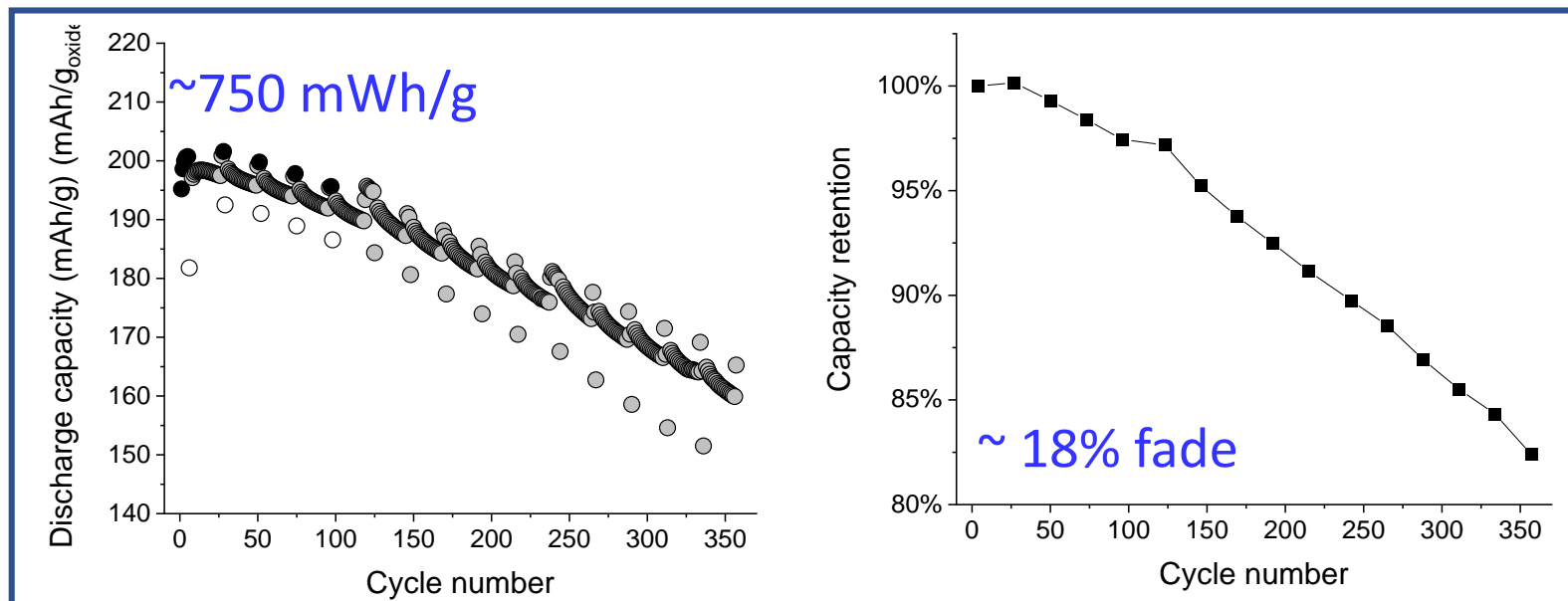
- Cell capacity and specific energy are lower than LiNi_{0.95}Co_{0.05}O₂ cell but can be increased by cycling full cell to 4.3 or 4.4 V
- Capacity fade and impedance rise are small relatively to that of the LiNi_{0.95}Co_{0.05}O₂//Gr cell



3-electrode cell data

- Cell impedance increase arises at the positive electrode.
- Negligible ASI changes at the negative electrode

LiNi_{0.9}Mn_{0.05}Co_{0.05}O₂//Gr cell: 3.0-4.2 V, 30°C, >350 cycles

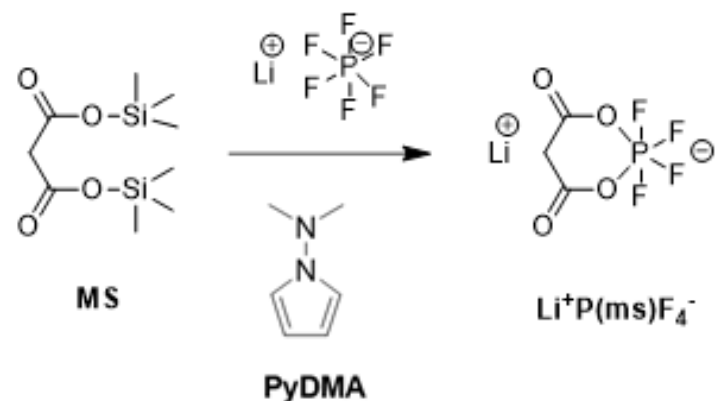


Electrochemical Performance

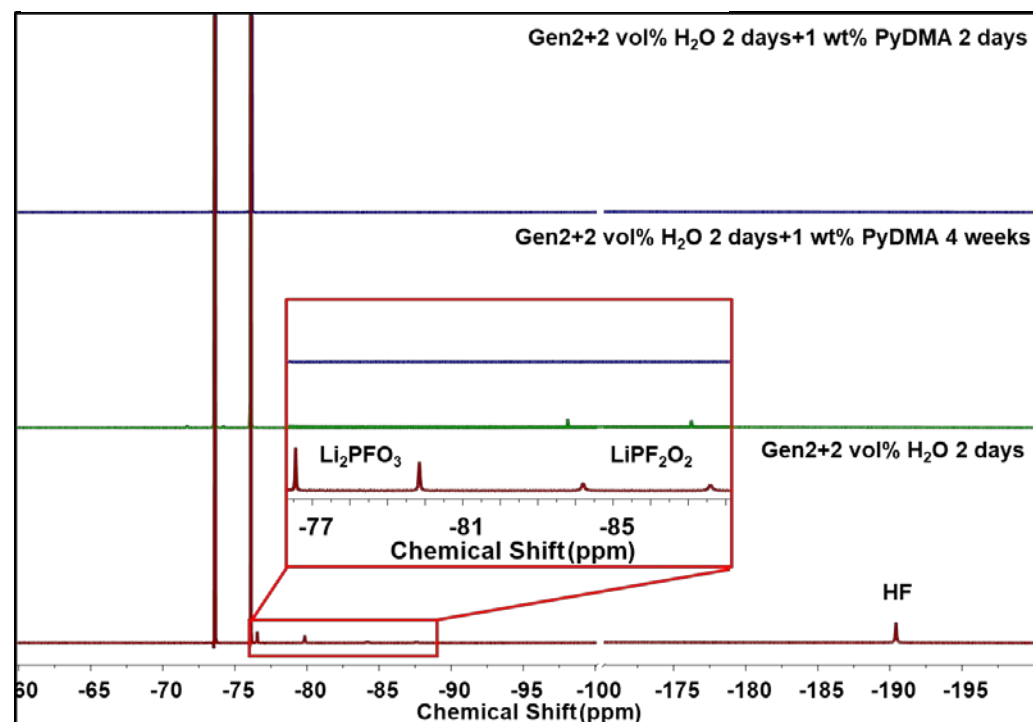
- Cell capacity and specific energy are comparable to those of LiNi_{0.95}Co_{0.05}O₂ cells
- Capacity fade and impedance rise are *much smaller* than those of LiNi_{0.95}Co_{0.05}O₂//Gr cells
- As in the other oxides, the positive electrode is the main contributor to cell impedance rise
- Even after > 350 cycles, the negative electrode ASI rise is negligible. This observation suggests that the graphite SEI remains a good conductor of Li⁺ ions

Best Performer

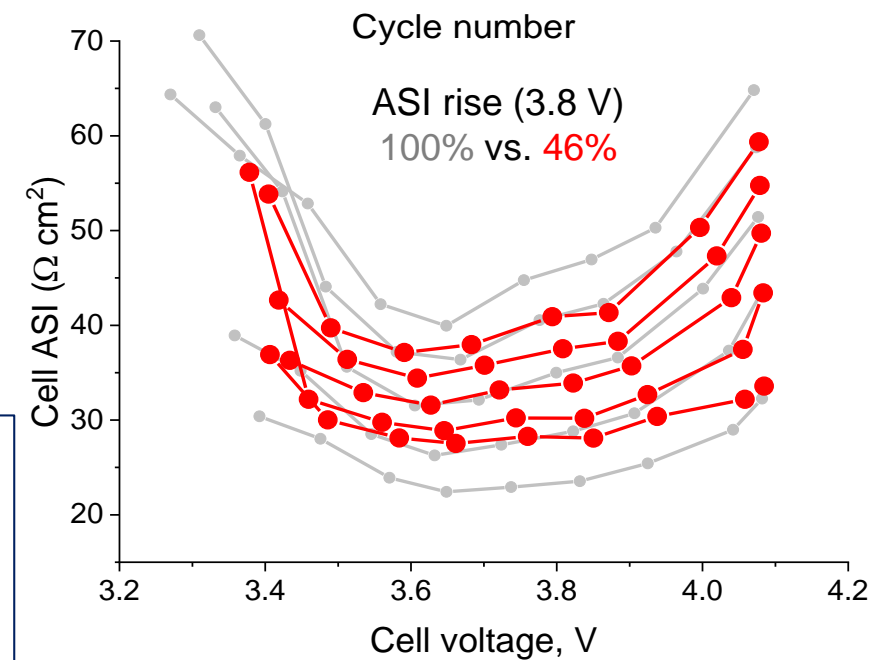
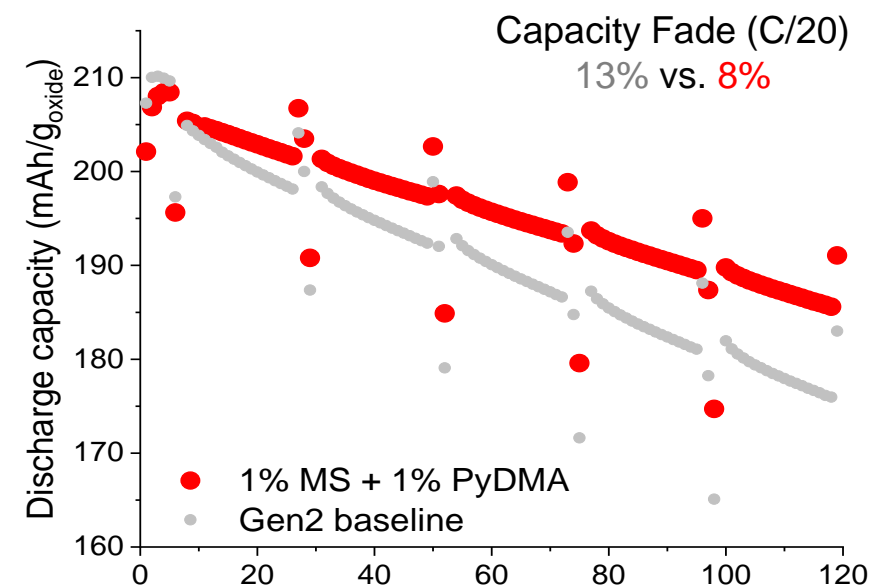
Enhancing $\text{LiNi}_{0.94}\text{Co}_{0.06}\text{O}_2//\text{Gr}$ performance with electrolyte additives: 3.0-4.2 V, 30°C



MS reacts with LiPF_6 *in situ* to form “beneficial” species.
PyDMA can remove HF formed by hydrolysis of Gen2 electrolyte.

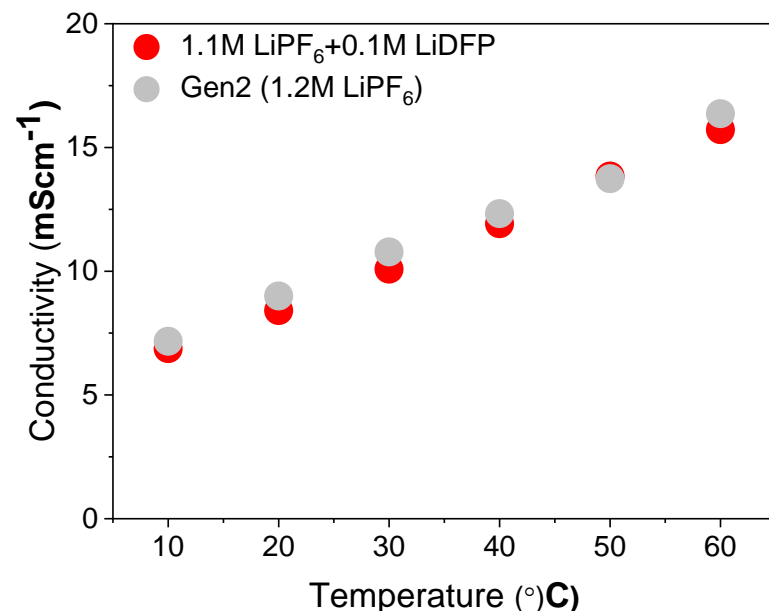


Combination of MS and PyDMA improves capacity retention and lowers impedance rise

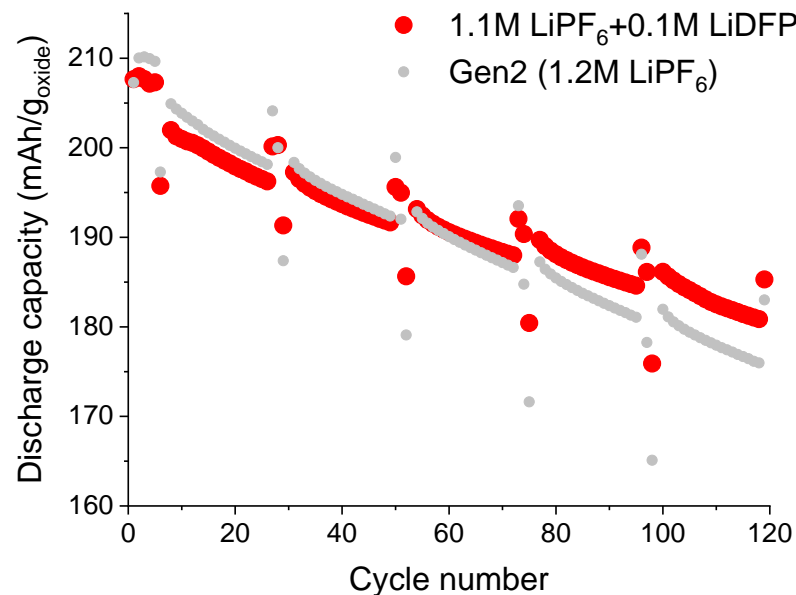


Suppressing impedance rise in $\text{LiNi}_{0.94}\text{Co}_{0.06}\text{O}_2//\text{Gr}$ cells using salt combinations in the electrolyte

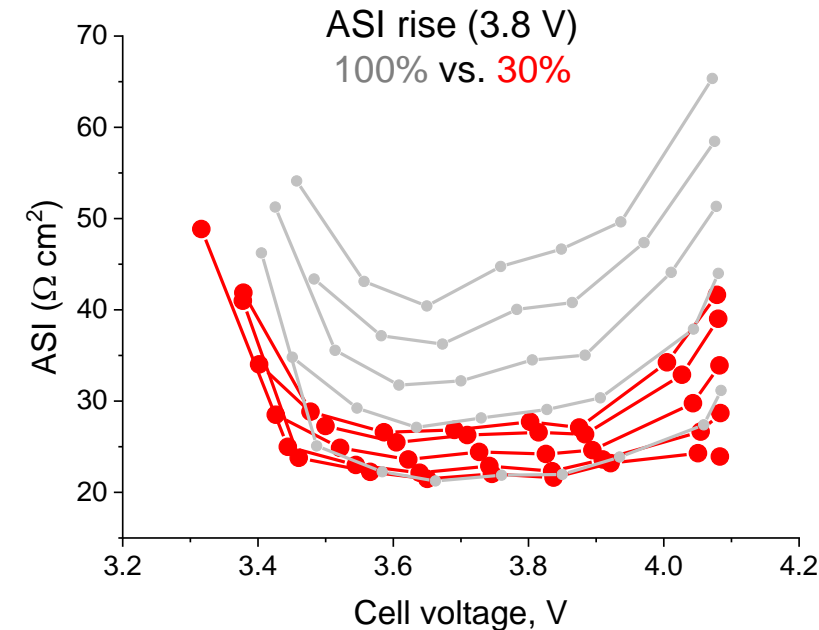
$\text{LiPF}_6 + \text{LiPF}_2\text{O}_2$ (LiDFP) dissolved in EC:EMC (3:7 wt/wt) solvent – 3.0 – 4.2 V, 30 °C tests



Conductivities similar for electrolytes with 1.1 M $\text{LiPF}_6 + 0.1\text{M}$ LiDFP or 1.2 M LiPF_6 (Gen 2 electrolyte)



Capacity fade similar for electrolytes with 1.1 M $\text{LiPF}_6 + 0.1\text{M}$ LiDFP or 1.2 M LiPF_6 (Gen 2 electrolyte)

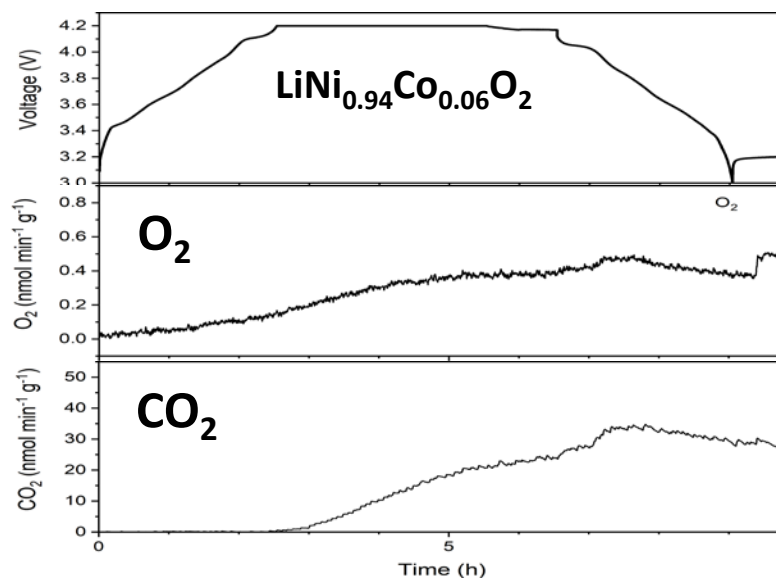
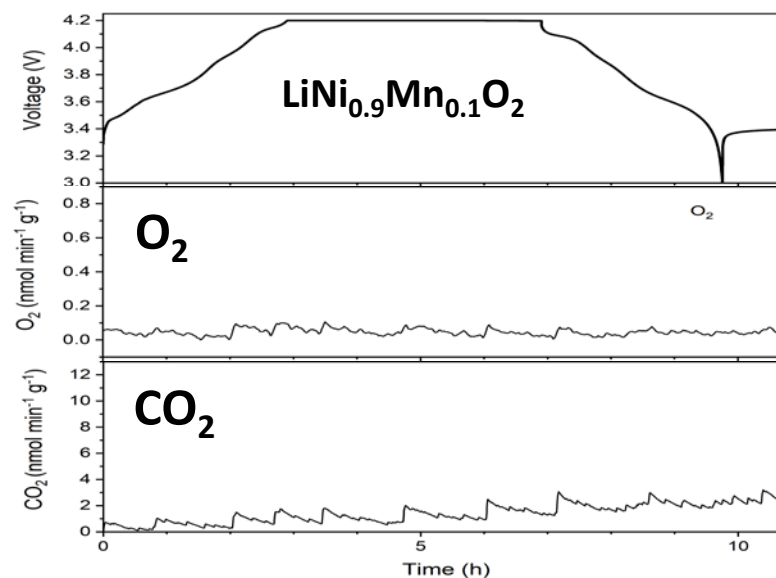
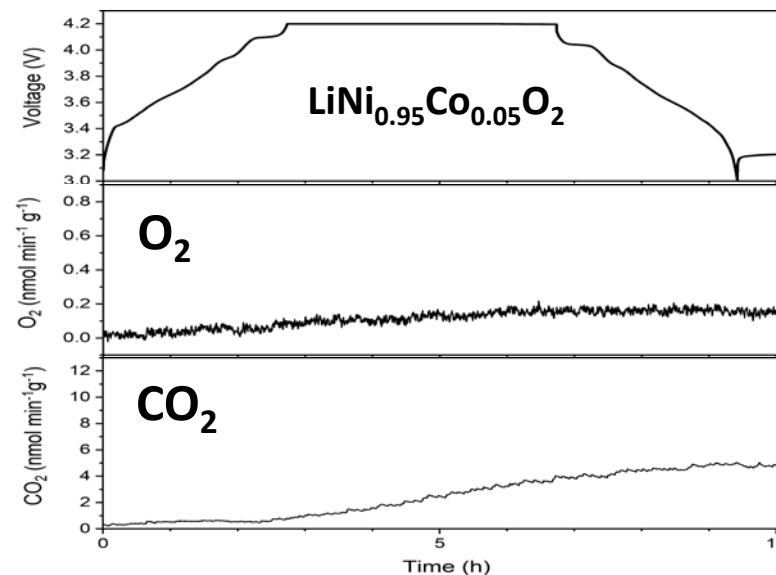
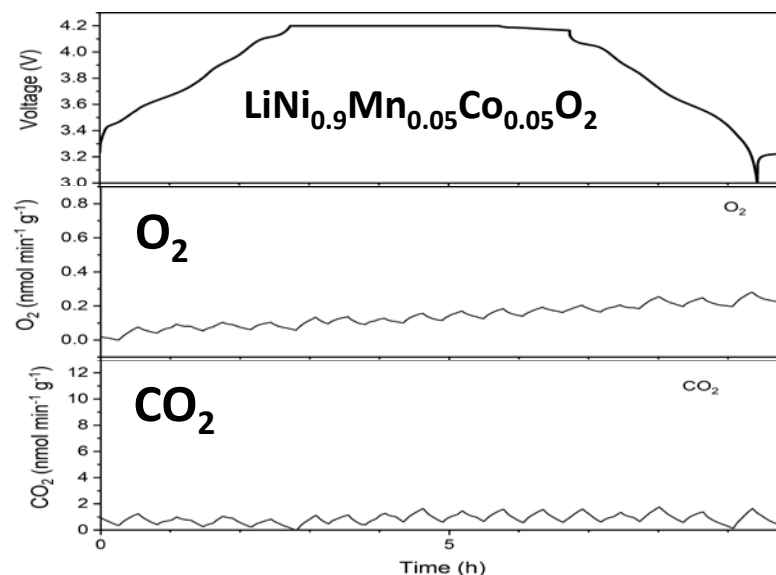


Impedance rise is significantly lower for the electrolytes with 1.1 M $\text{LiPF}_6 + 0.1\text{M}$ LiDFP

Electrolyte modifications can improve cell calendar and cycle life

Gas evolution in full cells with LNO-based oxide cathodes

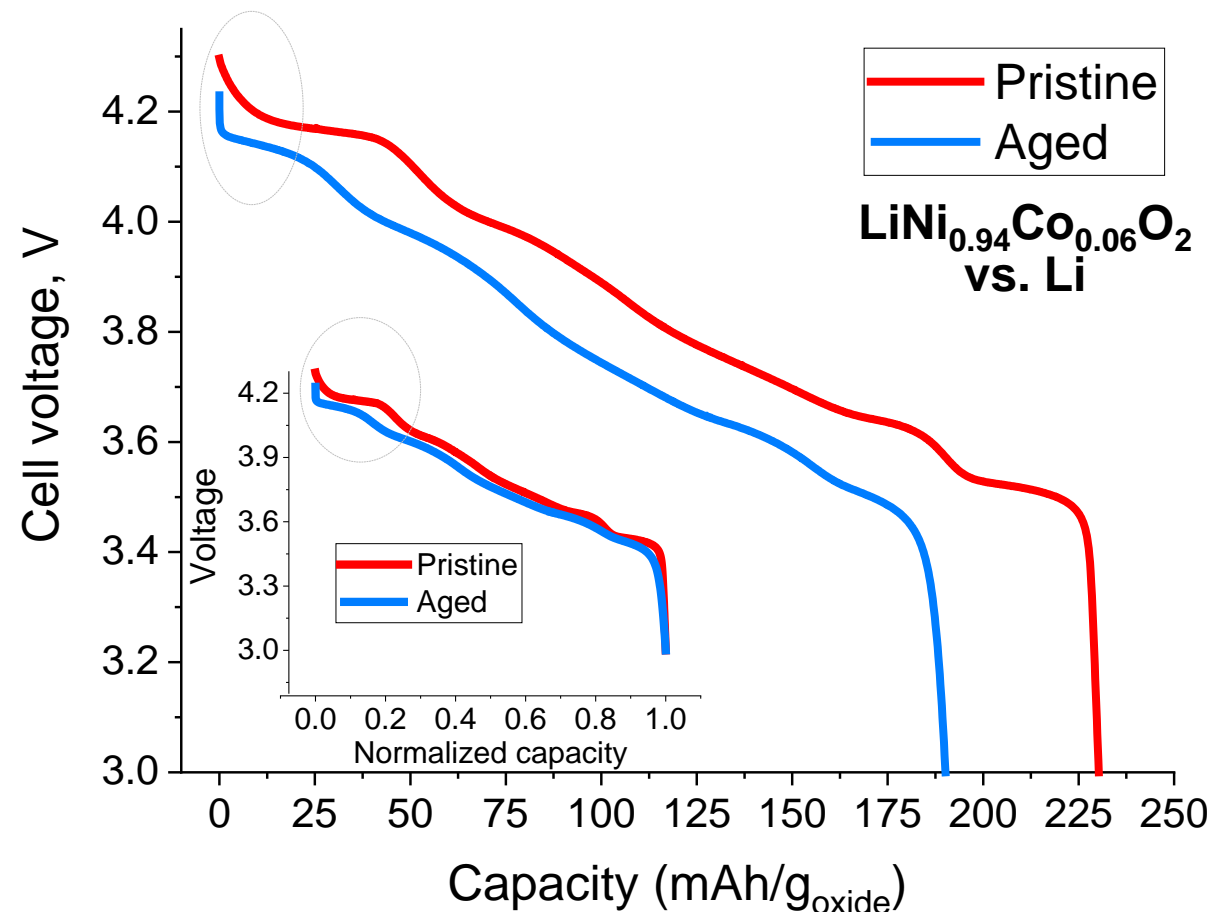
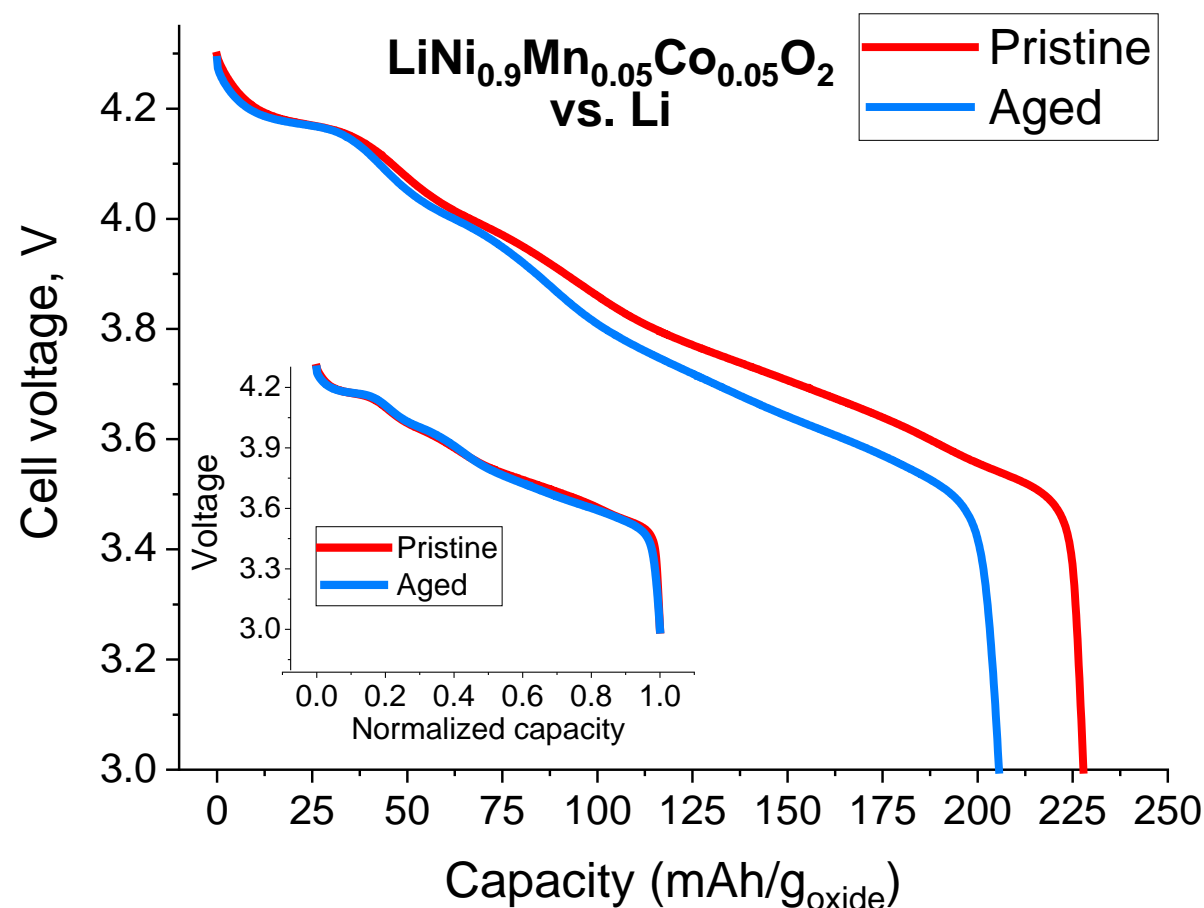
Differential Electrochemical Mass Spectroscopy (DEMS) is used to examine gas generation (3-4.2 V cycle)



- Significant amounts of O_2 and CO_2 are not observed for $\text{LiNi}_{0.9}\text{Mn}_{0.05}\text{Co}_{0.05}\text{O}_2$ and $\text{LiNi}_{0.9}\text{Mn}_{0.1}\text{O}_2$ cells during cycling
- Moderate CO_2 generation is observed for $\text{LiNi}_{0.95}\text{Co}_{0.05}\text{O}_2$ cell, mostly during the voltage hold
- O_2 release is clearly observed during voltage hold for the $\text{LiNi}_{0.94}\text{Co}_{0.06}\text{O}_2$ cell. Large amount of CO_2 is generated during the cycle. This gas generation could be associated with oxide synthesis conditions and the presence of carbonate impurities on the surface.

Harvested cathode electrochemistry: 3.0-4.3 V, 30°C, C/100

Electrodes harvested from full cells after ~350 cycles

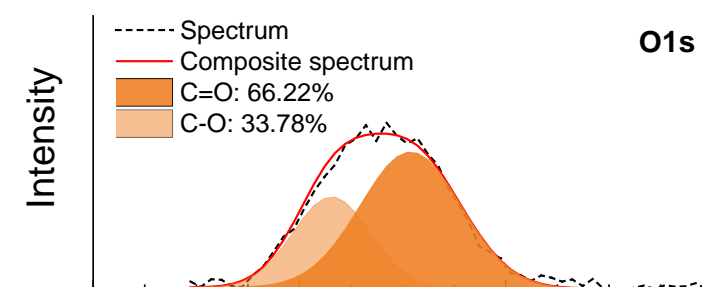
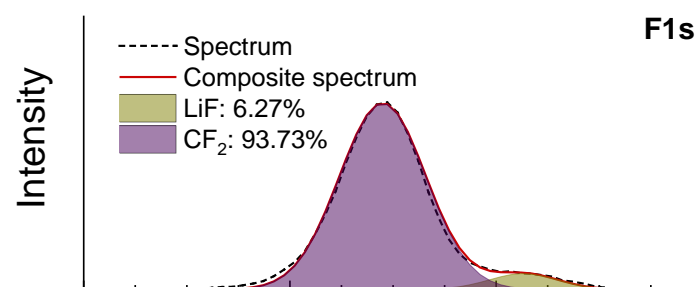
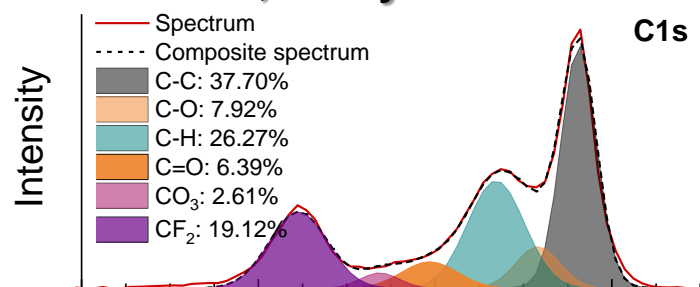


Capacity loss of LiNi_{0.94}Co_{0.06}O₂ > LiNi_{0.95}Mn_{0.05}Co_{0.05}O₂. “Normalized-capacity” plots suggest crystallographic changes in LiNi_{0.94}Co_{0.06}O₂ but not in LiNi_{0.95}Mn_{0.05}Co_{0.05}O₂.

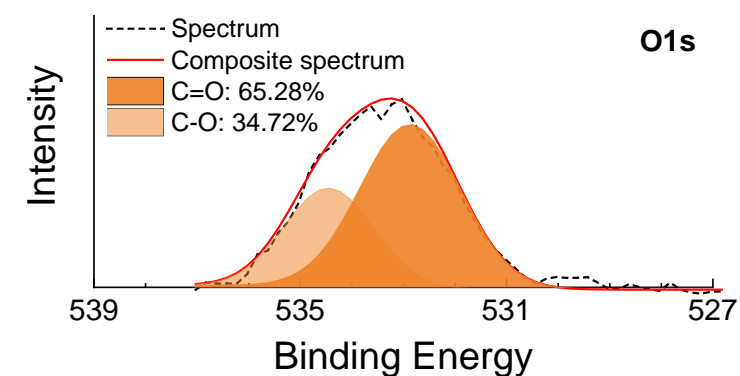
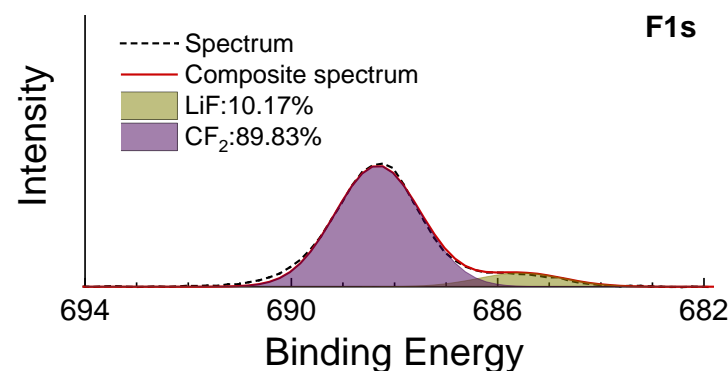
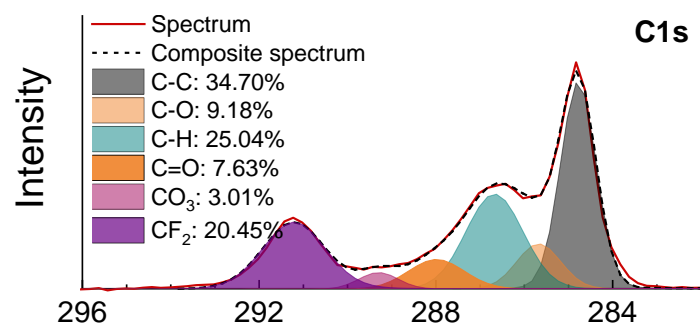
Harvested cathode XPS show aging-related surface-changes

X-ray photoelectron spectroscopy data from $\text{LiNi}_{0.94}\text{Co}_{0.06}\text{O}_2//\text{Gr}$ cells with Gen2 electrolyte

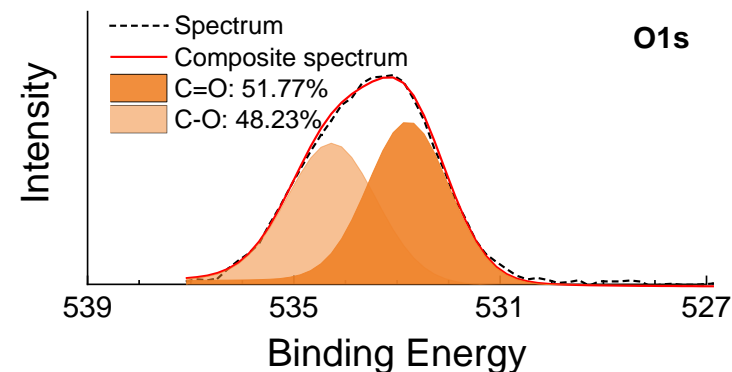
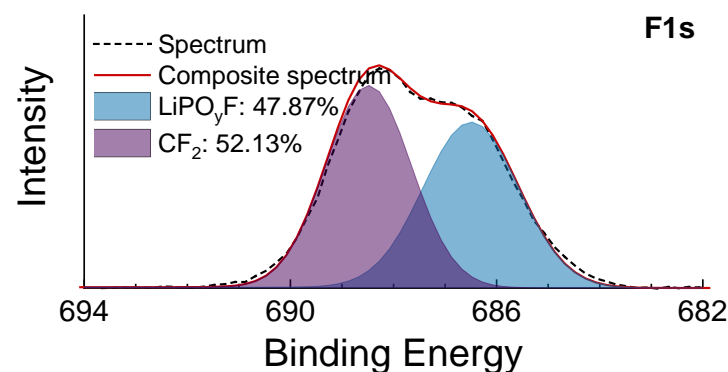
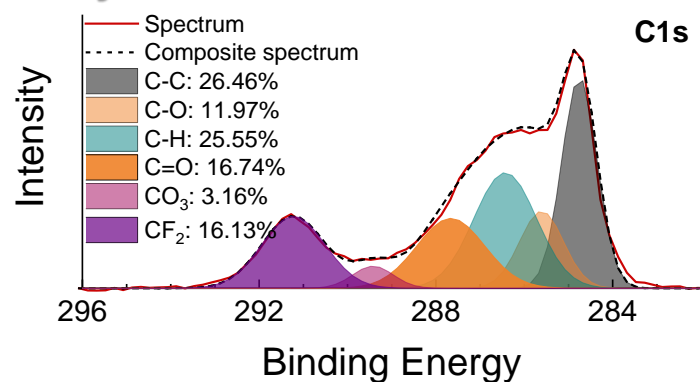
After formation, ~ 4 cycles



~120 cycles



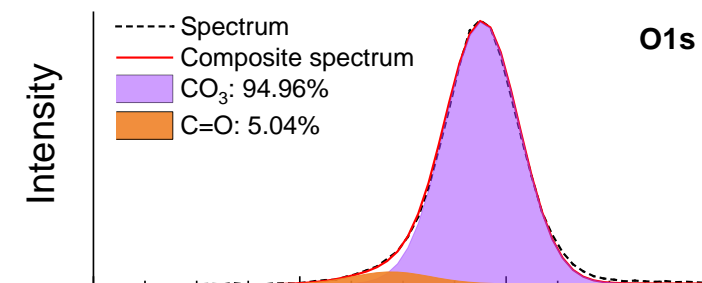
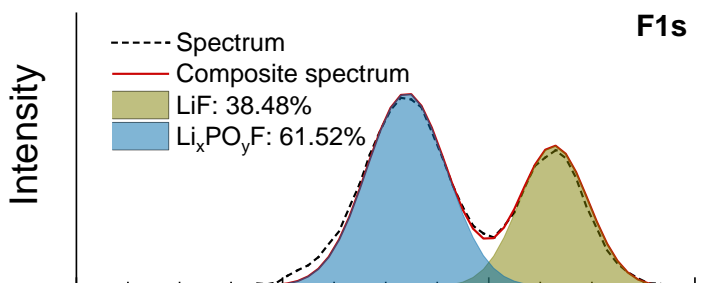
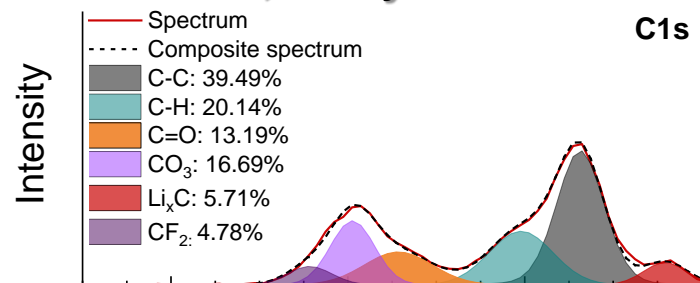
> 350 cycles



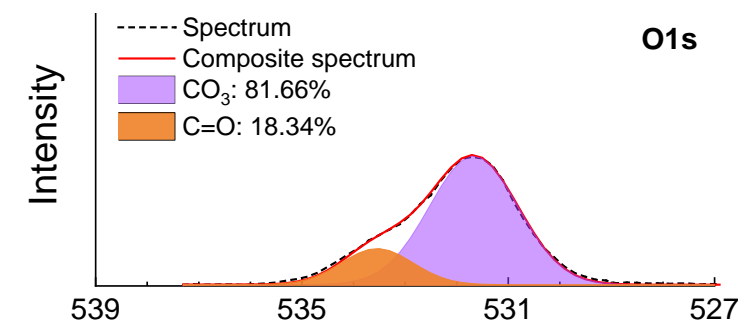
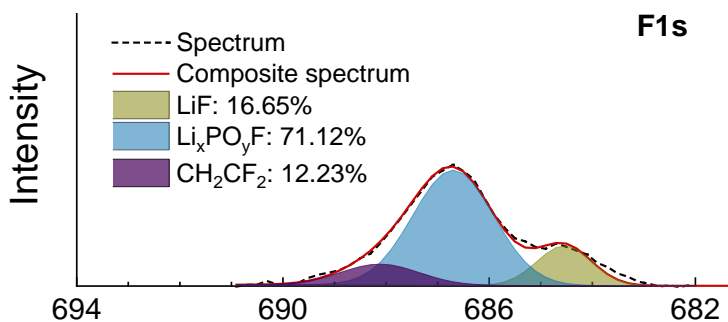
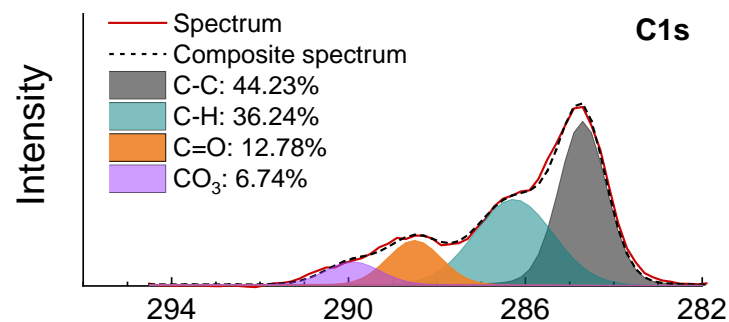
Harvested anode XPS show aging-related SEI changes

X-ray photoelectron spectroscopy data from $\text{LiNi}_{0.94}\text{Co}_{0.06}\text{O}_2//\text{Gr}$ cells with Gen2 electrolyte

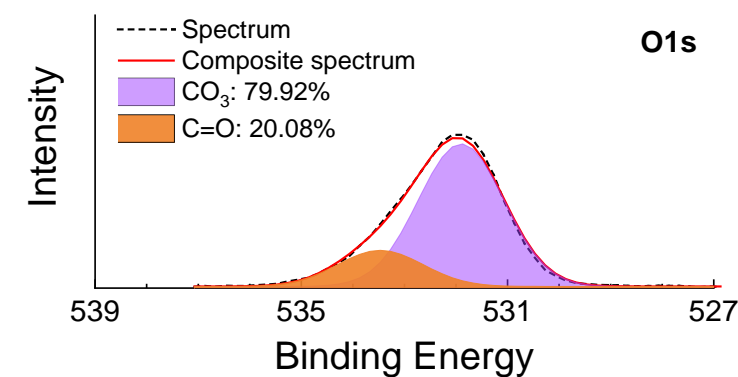
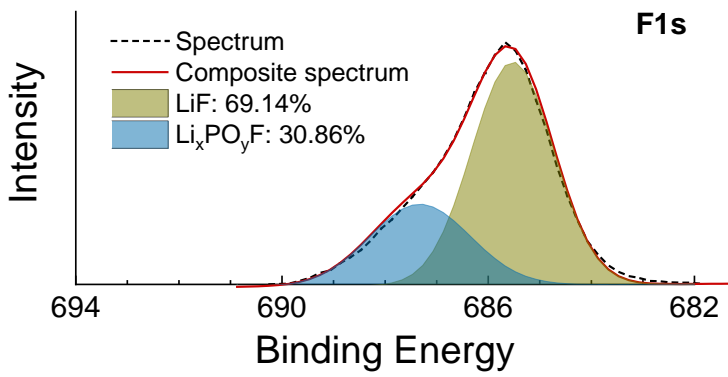
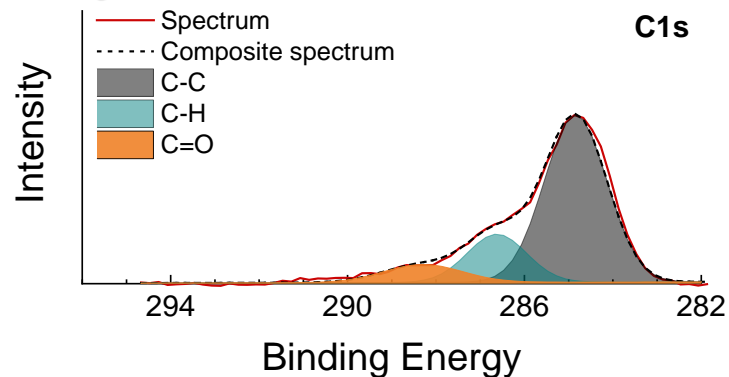
After formation, ~ 4 cycles



~ 120 cycles

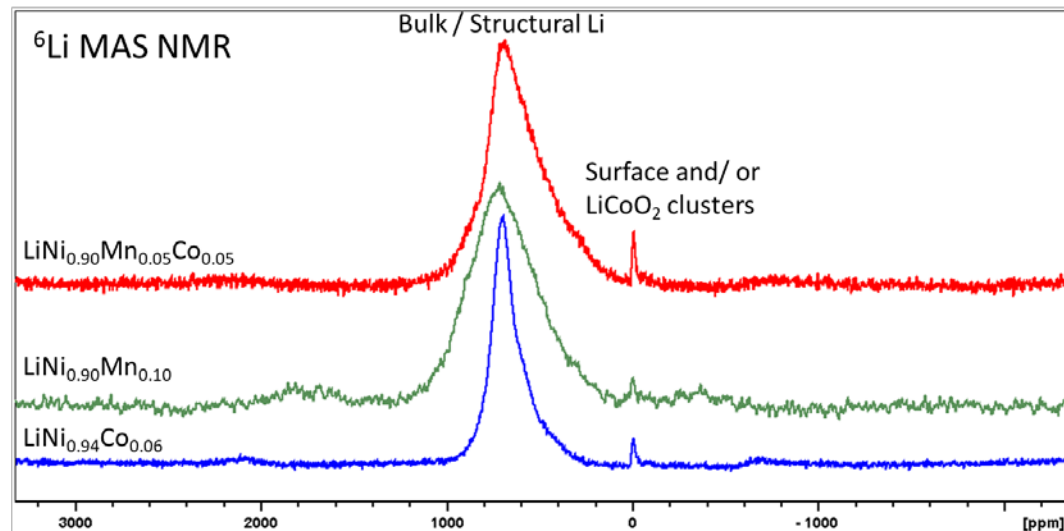


> 350 cycles



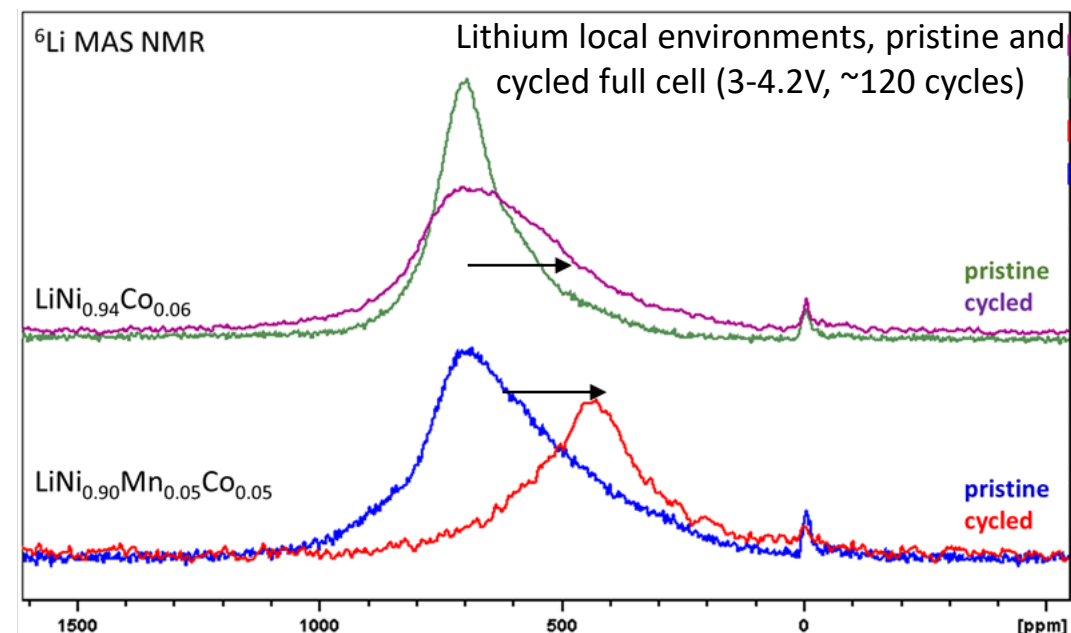
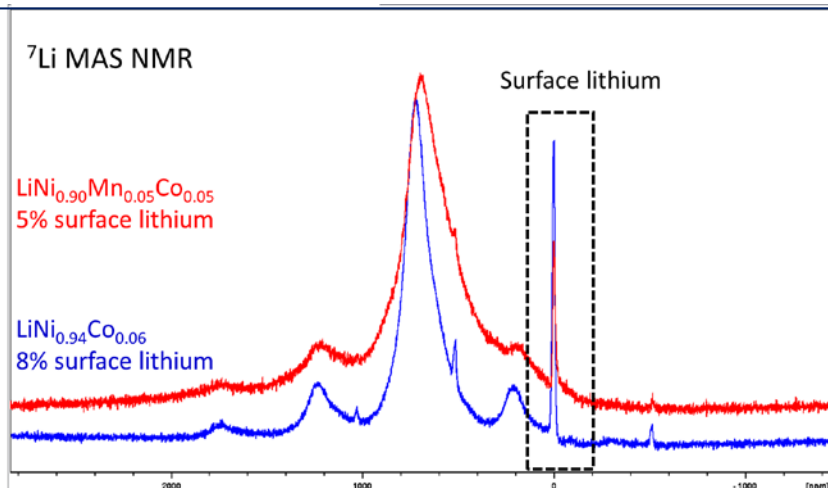
Structural analysis of oxide cathodes by solid state NMR

Solid State NMR is used to directly observe bulk and surface lithium environments within different oxide compositions and to determine structure changes that occur during cycling



Introduction of Mn in the oxide bulk broadens ⁶Li NMR peaks, suggesting more structural disorder and partial randomization of transition metal distribution. No Mn clustering is observed.

Surface lithium quantified via ⁷Li NMR.
LiNi_{0.94}Co_{0.06} shows highest surface Li content (8%)

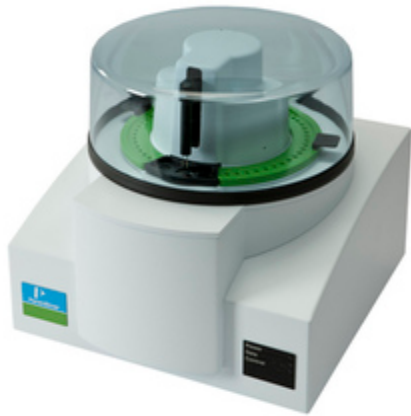


Cycled samples show ⁶Li NMR peak shifts due to increase in the oxide's average TM oxidation state that results from a decrease in its Li content during cycling. Peak width decrease for LiNi_{0.90}Mn_{0.05}Co_{0.05} suggests higher Li mobility.

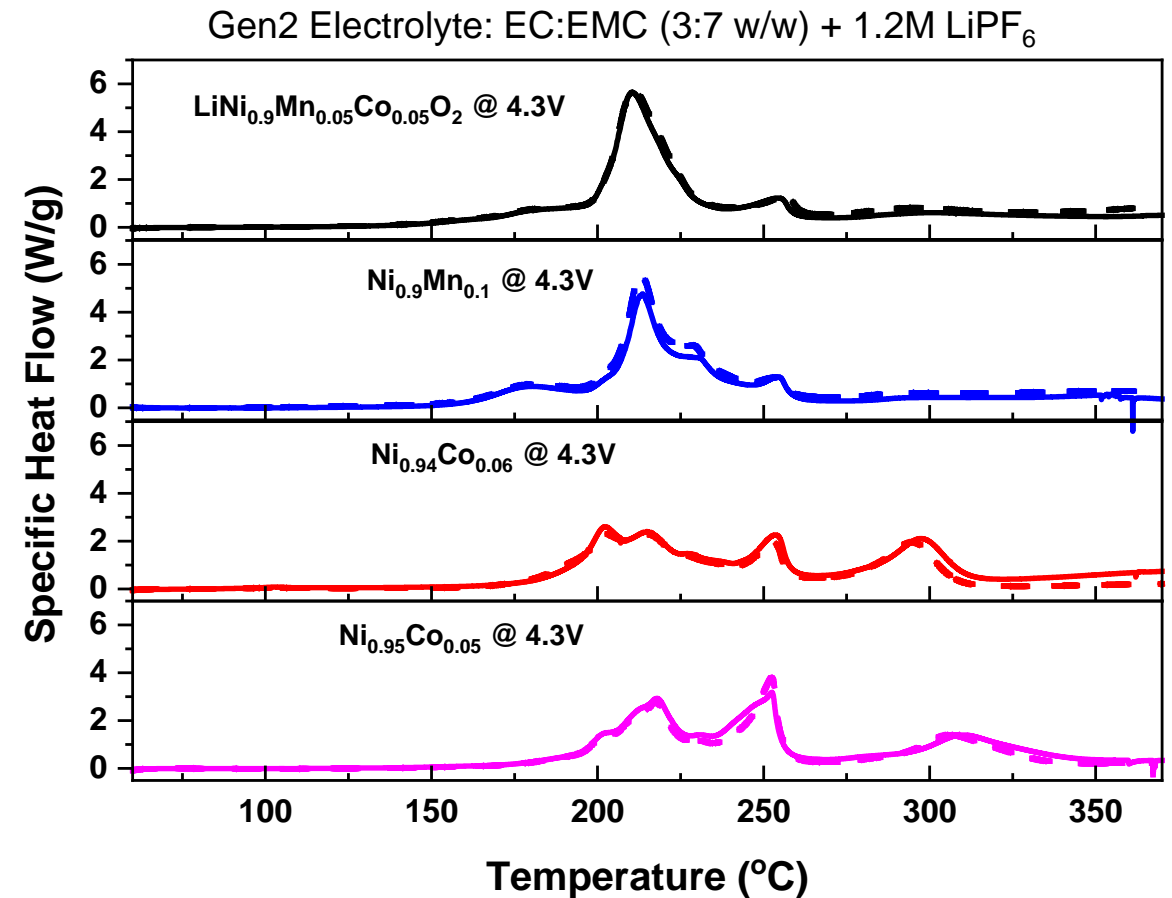
Differential scanning calorimetry (DSC) of delithiated oxides

DSC data are used to evaluate the life and safety characteristics of battery materials

- After 3 formation cycles at C/10 rate, the oxide-electrode was charged to 4.3 V vs. Li/Li⁺
- Recovered electrode material was mixed with Gen2 electrolyte and sealed in sample holder
- DSC scan was from 50°C to 370°C at 5°C/min



Reusable Steel High Pressure Capsules, from Perkin Elmer



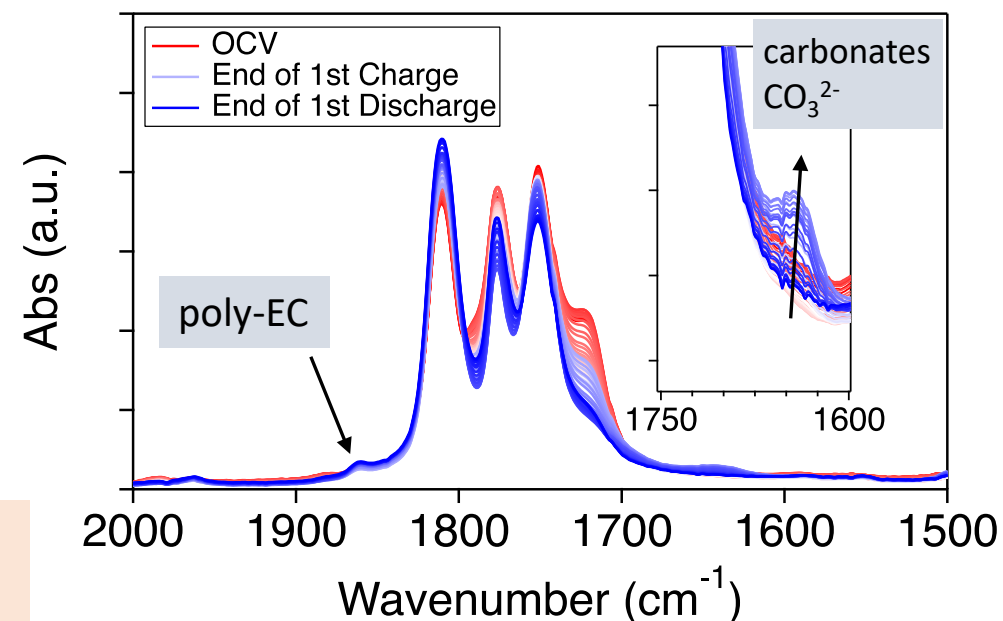
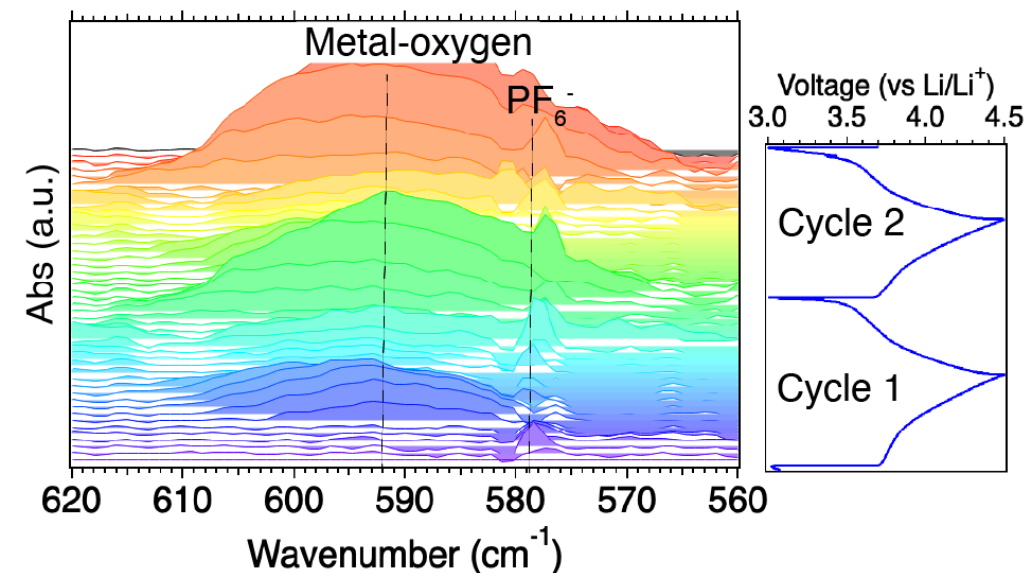
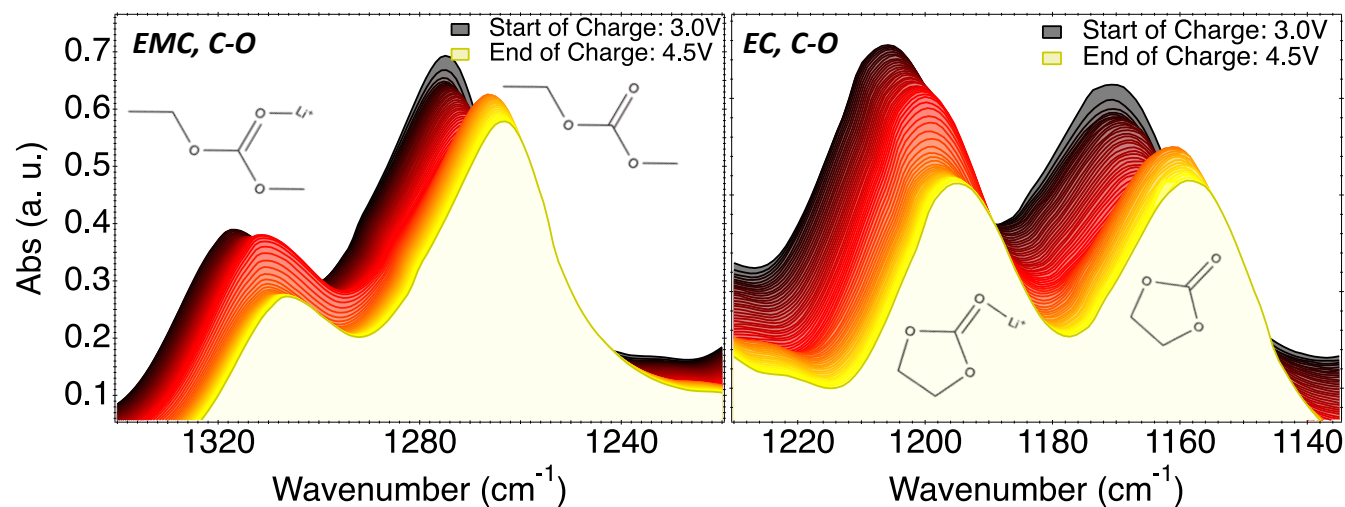
Multi-exothermic peaks are observed for all 4 charged oxide active materials
Total heat generations of all 4 oxide samples are similar to each other

In situ spectroscopic analysis of oxide-electrolyte interfaces

Data from NMC622 vs. Li cells

In situ ATR-FTIR cells show repeatable electrochemical performance and strong FTIR vibrational absorption signals at cathode surface

- Near-surface (de)solvation (ions–solvent molecules) changes during galvanostatic cycling (C/10, 3.0-4.5 V vs Li/Li⁺) observed in Gen2 electrolyte (1.2 M LiPF₆ in EC:EMC, 3:7 wt%)
- NMC622 cathode metal-oxygen vibrational absorptions are sensitive to local order and Li⁺ vacancies
- Evolution of cathode-electrolyte interphase (CEI) components seen

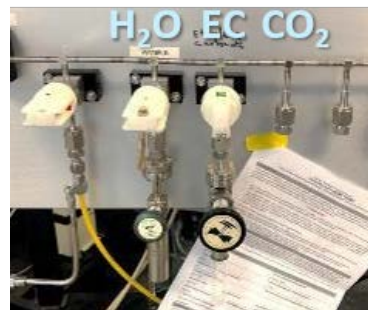
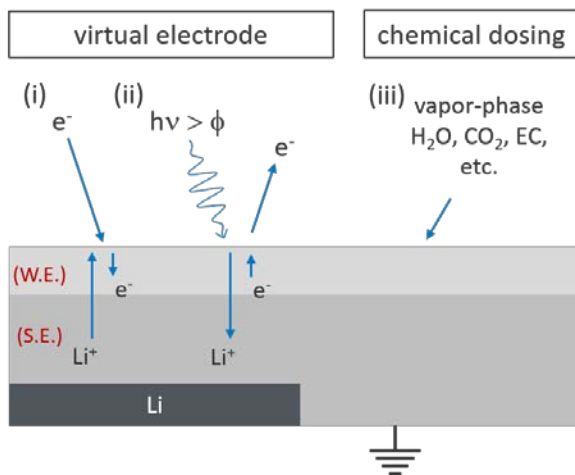


Have measured **characteristic FTIR peak signatures** (e.g., position, shift, and intensity) of **electrolyte, cathode, and CEI** in case study of NMC622

In situ XPS to study surface chemistry of LNO-based oxides

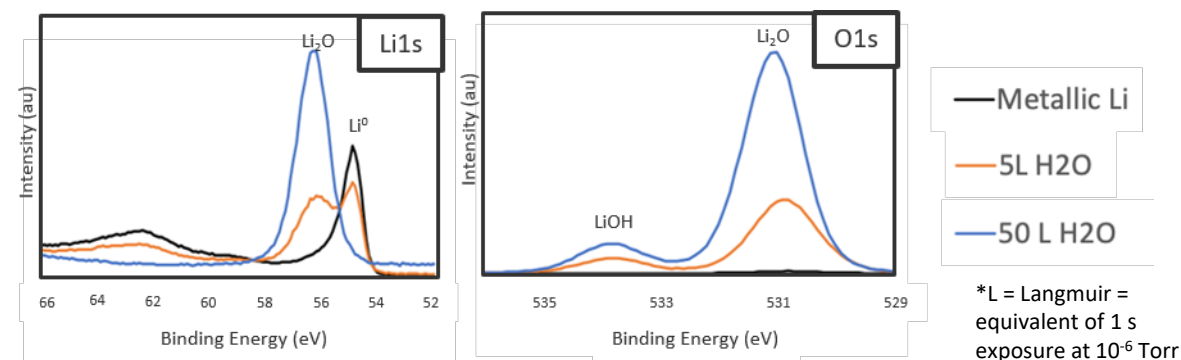
In situ XPS is used to evaluate surface reactivities of LNO-based oxide materials to environmental and electrolyte molecules

- To validate the *in-situ* gas-dosing approach for surface study, H₂O molecule were dosed to Li metal surface up to 50 Langmuir
- H₂O was dosed to LiNiO₂ up to 100 Langmuir

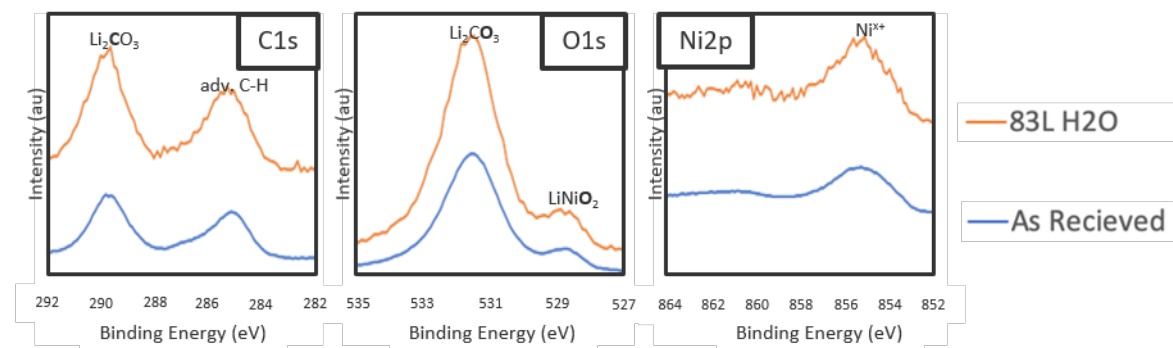


Proof-of-concept test with Li metal

XPS of metallic Li before and after H₂O dosing



XPS of LiNiO₂ before and after H₂O dosing



H₂O quickly reacts with Li metal and forms Li₂O that completely passivates Li
 Li₂CO₃ on LiNiO₂ seems to increase with H₂O dosing
 Sputtering to clean the surface of LiNiO₂ creates metallic Ni

Response to Previous Year's Reviewer Comments

- This project was not reviewed in the previous year

Next-Gen Cathode Project Contributors

Collaboration and Coordination

- | | | |
|------------------------------|----------------------------|--------------------------------|
| ▪ Daniel Abraham | ▪ Sang-Don Han | ▪ Yan Qin |
| ▪ Khalil Amine | ▪ Kevin Hays | ▪ Yang Ren |
| ▪ Mahalingam Balasubramanian | ▪ Hakim Iddir | ▪ Marco Rodrigues |
| ▪ Ilias Belharouak | ▪ Andrew Jansen | ▪ Aryal Shankar |
| ▪ Ira Bloom | ▪ Christopher Johnson | ▪ Boyu Shi |
| ▪ Anthony Burrell | ▪ Ozge Kahvecioglu Feridun | ▪ Woochul Shin |
| ▪ Guoying Chen | ▪ Minkyung Kim | ▪ Ilya Shkrob |
| ▪ Jiajun Chen | ▪ Joel Kirner | ▪ Seoung-Bum Son |
| ▪ Lina Chong | ▪ Eungje Lee | ▪ Adam Tornheim |
| ▪ Devika Choudhury | ▪ Linze Li | ▪ Stephen Trask |
| ▪ Jason Croy | ▪ Chen Liao | ▪ Bertrand Tremolet de Villers |
| ▪ Dennis Dees | ▪ Qian Liu | ▪ John Vaughey |
| ▪ Fulya Dogan | ▪ Wenquan Lu | ▪ Anh Vu |
| ▪ Alison Dunlop | ▪ Jun Lu | ▪ Chongmin Wang |
| ▪ Jessica Durham | ▪ Mei Luo | ▪ Jianzhong Wang |
| ▪ Jeff Elam | ▪ Anil Mane | ▪ David Wood |
| ▪ Sarah Frisco | ▪ Jagjit Nanda | ▪ Zhenzhen Yang |
| ▪ Juan Garcia | ▪ Kyusung Park | ▪ Junghoon Yang |
| ▪ Linxiao Geng | ▪ Nate Phillip | ▪ Jianzhong Yang |
| ▪ Jihyeon Gim | ▪ Bryant Polzin | ▪ Haotian Zheng |
| ▪ Arturo Gutierrez | ▪ Krzysztof Pupek | ▪ Lianfeng Zhou |

Major Research Facilities

- | | | |
|---|--|---|
| ▪ Materials Engineering Research Facility | ▪ Advanced Light Source | ▪ National Energy Research Scientific Computing Center (LBNL) |
| ▪ Post-Test Facility | ▪ Battery Manufacturing Facility | ▪ Stanford Synchrotron Radiation Light Source |
| ▪ Cell Analysis, Modeling, and Prototyping | ▪ Advanced Photon Source (APS) | |
| ▪ Spallation Neutron Source | ▪ Laboratory Computing Resource Center (ANL) | |
| ▪ Environmental Molecular Sciences Laboratory | ▪ NMR Spectroscopy Lab (ANL) | |

Support for this work from the ABR Program, Office of Vehicle Technologies, DOE-EERE, is gratefully acknowledged – Peter Faguy, David Howell

Proposed Future Research

- Continue ongoing diagnostic tests and determine performance degradation mechanisms
 - Electrochemical (3-electrode cells, symmetric cells) and physicochemical (XRD, NMR, TEM/STEM, XAS, gas analysis, etc.) tests will continue to provide valuable information
 - Continue development of *in situ/operando* diagnostic techniques
- Scale-up additional oxide compositions and evaluate using standard protocols
 - Identify compositions with little or no cobalt that perform as well or better than NMC622
 - Examine compositions that have higher Mn content, such as derivatives of $\text{LiNi}_{0.5}\text{Mn}_{0.5}\text{O}_2$
- Develop oxide particle coatings and new electrolytes to mitigate performance loss
 - Identify coating techniques that can be easily scaled-up
 - Find electrolyte systems that show improved performance in thermal abuse tests
- Establish electrochemical models to explain performance of low-Co oxide systems
 - Models are needed to explain changes in interfacial transport and kinetic parameters with SEI and surface modifications, explain parasitic currents during calendar-life holds, etc.

Any future work is subject to change depending on funding levels

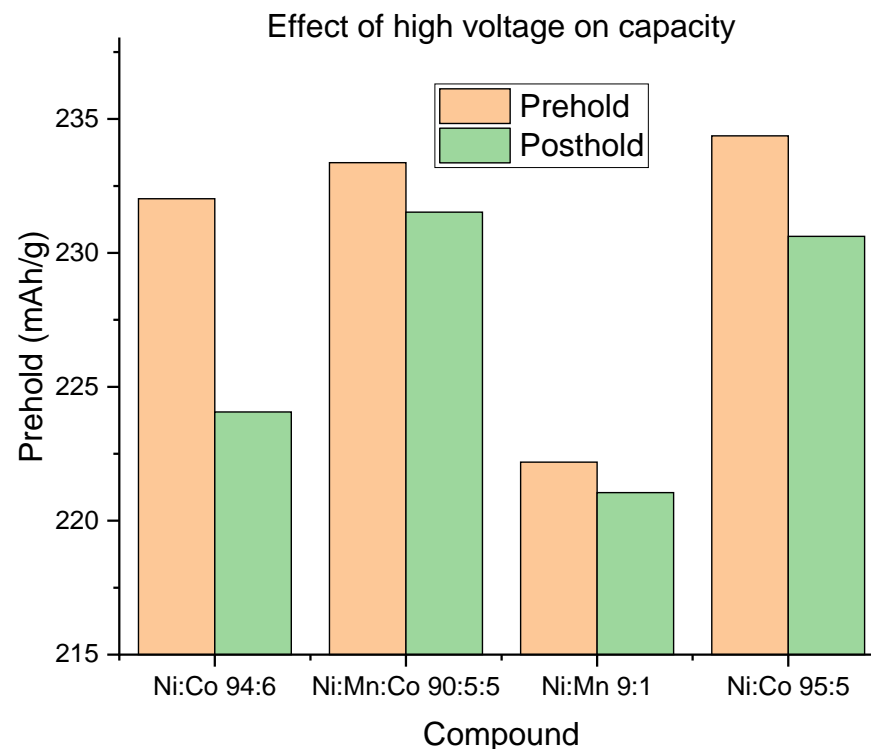
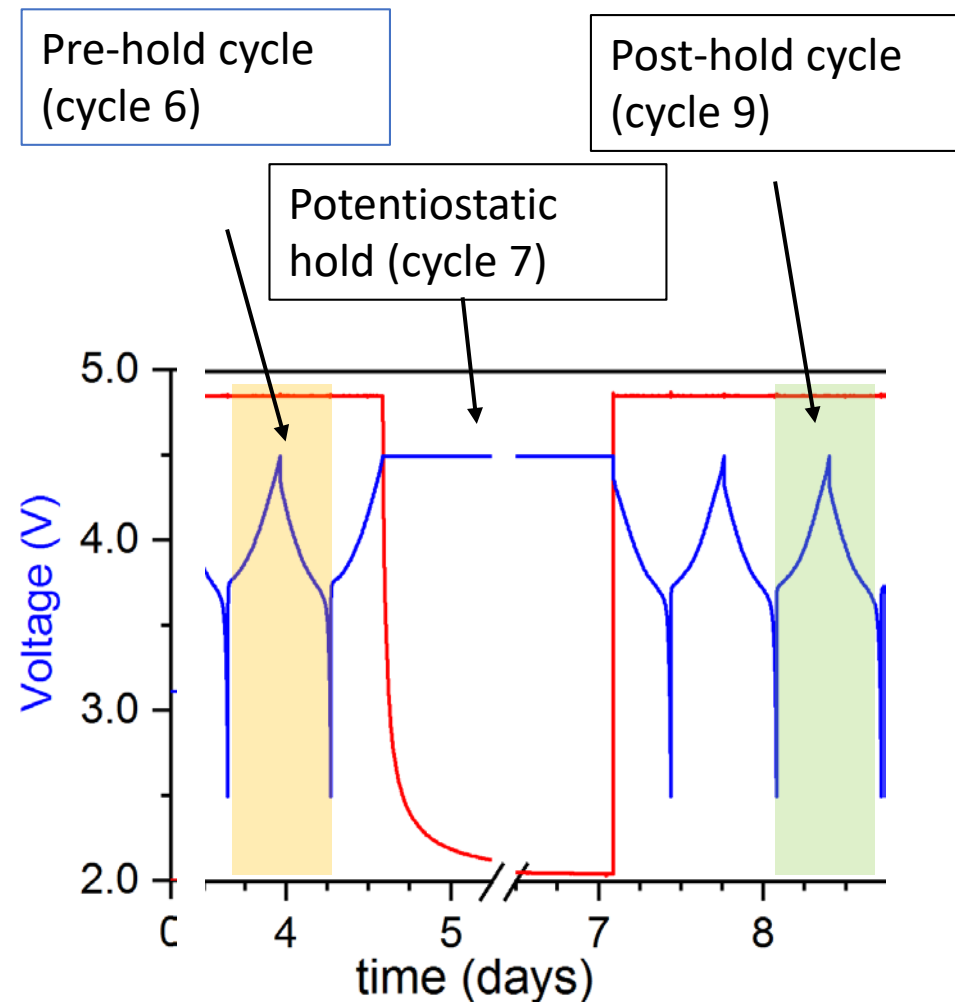
Summary

- Low Co oxides that are variants of LiNiO_2 have been synthesized and scaled up to ~100 g levels
 - Diagnostic tests conducted on CAMP-fabricated electrodes containing $\text{LiNi}_{0.94}\text{Co}_{0.06}\text{O}_2$, $\text{LiNi}_{0.95}\text{Co}_{0.05}\text{O}_2$, $\text{LiNi}_{0.9}\text{Mn}_{0.1}\text{O}_2$ and $\text{LiNi}_{0.90}\text{Mn}_{0.05}\text{Co}_{0.05}\text{O}_2$
- Half-cell and Full-cell standardized cycling protocols developed to examine these oxide materials
 - Electrochemical cycling data from full cells indicate that $\text{LiNi}_{0.90}\text{Mn}_{0.05}\text{Co}_{0.05}\text{O}_2$ and $\text{LiNi}_{0.9}\text{Mn}_{0.1}\text{O}_2$ show higher capacity retention and lower impedance rise than $\text{LiNi}_{0.95}\text{Co}_{0.05}\text{O}_2$ and $\text{LiNi}_{0.94}\text{Co}_{0.06}\text{O}_2$
- Tests in Reference-electrode cells indicate source of impedance rise
 - Oxide-positive electrode is the dominant contributor; negligible ASI rise at the graphite-negative electrode
- Tests with harvested-electrode indicate oxide particle isolation and structure changes
 - Evidence for bulk-crystallographic changes in $\text{LiNi}_{0.94}\text{Co}_{0.06}\text{O}_2$ but not in $\text{LiNi}_{0.90}\text{Mn}_{0.05}\text{Co}_{0.05}\text{O}_2$
- Gas analysis studies reveal oxygen evolution from some oxides
 - Oxygen evolution observed for $\text{LiNi}_{0.94}\text{Co}_{0.06}\text{O}_2$ but not $\text{LiNi}_{0.90}\text{Mn}_{0.05}\text{Co}_{0.05}\text{O}_2$ or $\text{LiNi}_{0.9}\text{Mn}_{0.1}\text{O}_2$
- New electrolyte compositions show promise for improving capacity and power retention
 - Tests using *in situ* synthesized compounds, HF getters, and dual salt electrolytes
- Solid state NMR, Differential scanning calorimetry, X-ray photoelectron spectroscopy, *in situ* FTIR, *in situ* Raman and *in situ* XPS methodologies have also been developed
 - Data from these tests are being used to identify mechanisms associated with oxide performance loss and to develop low-Co oxides that meet energy density, power density, life and safety goals of the program

Technical Backup Divider Slide

Using Protocols: Pre- and Post-hold capacities

Pre- and Post-hold capacities give insight into cathode damage/activation



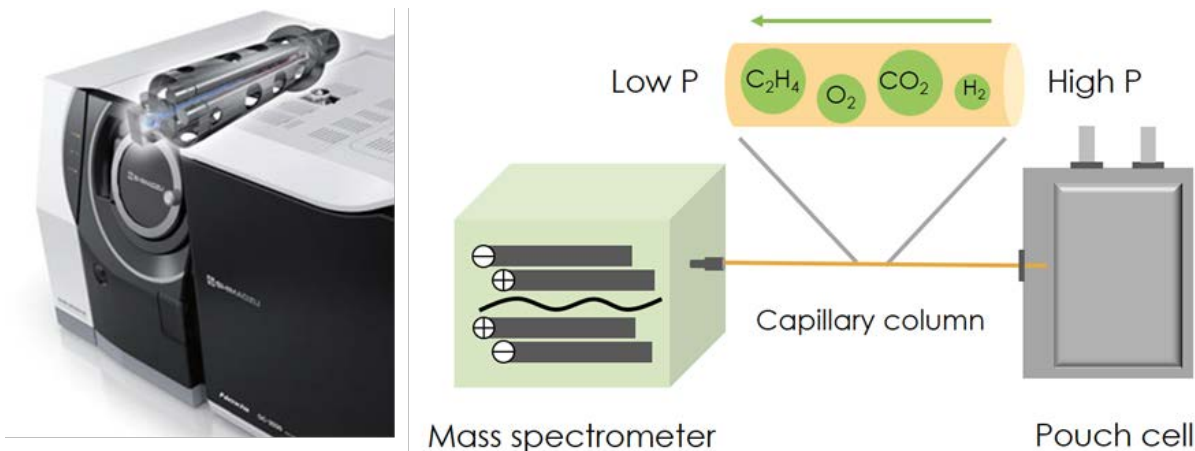
High-voltage holds can degrade the electrolyte and the cathode. Cathode stability is probed by evaluating the discharge capacity both before (Prehold) and after (Posthold). Large differences indicate more damage.

Ni:Co compounds lose more capacity after subjected to 4.5 V hold than Mn-containing compounds

Gas Analysis methodology

Differential Electrochemical Mass Spectroscopy (DEMS) is used to investigate interfacial stability of oxide-cathodes by studying the gases generated during electrode-electrolyte reactions

- Gases generated are directly sampled into quadrupole mass spectroscopy from pouch cells and analyzed in a real-time manner.
- Electrochemical testing conditions can be easily controlled in terms of C-rate, upper-cut off voltages, temperature, etc.
- Standardized protocols have been developed to compare gas generation results among different cathode materials.
- Gas concentration is calibrated using standard gases.



Pouch Cell configuration

Cathode: LNO-based oxides

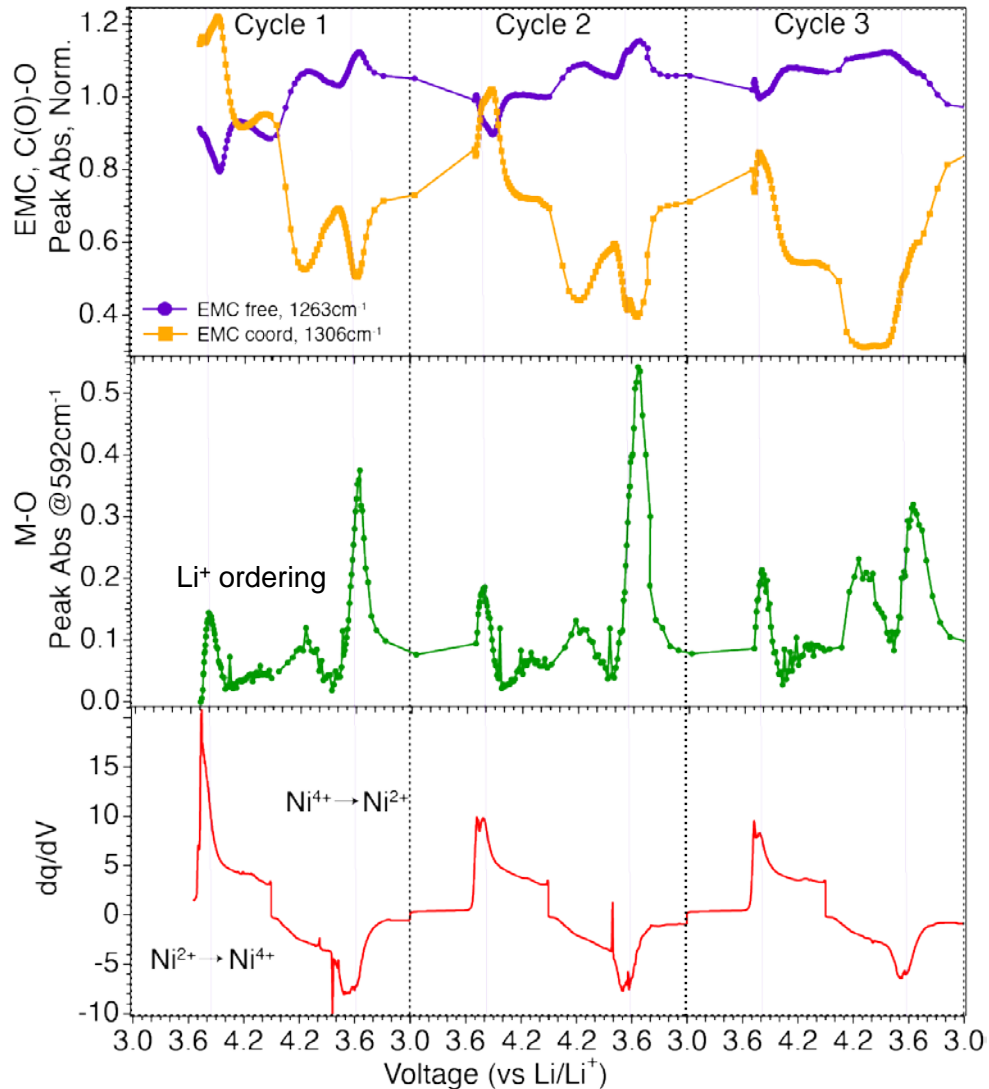
Anode: Graphite (SLC1506)

Electrolyte: 1.2M $LiPF_6$ in EC:EMC (3:7 w/w)

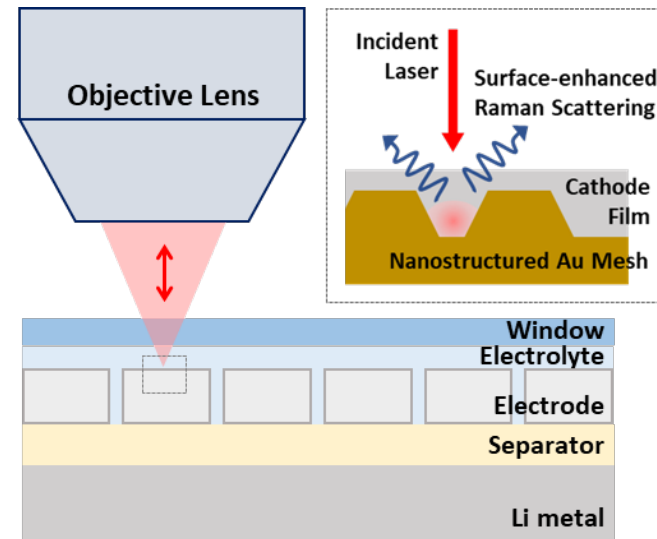
Fill factor: 3x pore volume

In situ Spectroscopic Analysis of Model NMC622 Cathode

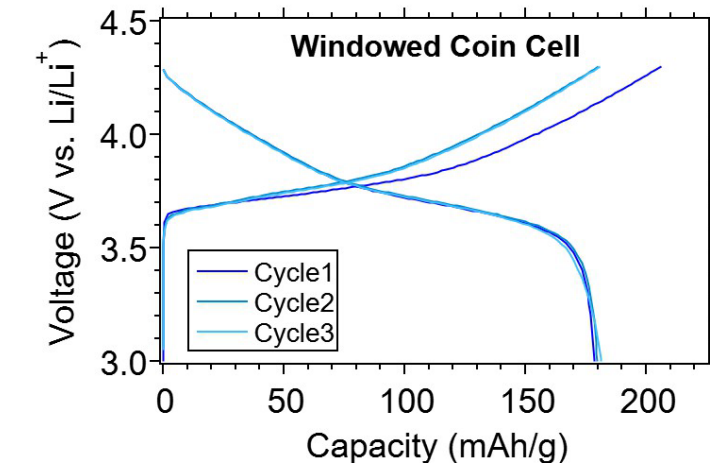
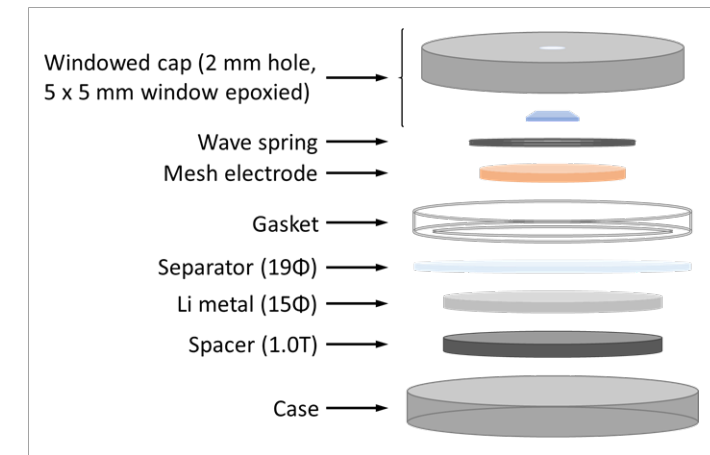
Correlation of solvent structure, cation ordering and cathode redox behavior (by ATR-FTIR)



In situ Raman/SERS analysis with a newly developed cell



- Develop a windowed coin cell and surface-enhanced Raman spectroscopy (SERS) technique.
- Demonstrate reliable/repeatable electrochemical performance with a NMC622 on Al mesh/Li half cell (C/10, 3-4.3 V in Gen2).



Have correlated **specific cathode chemistries** (e.g., transition metal redox and oxygen evolution) to **FTIR signatures** using complimentary techniques (e.g., Raman).

Selected Recent Publications

Geng et al. , "High Accuracy In-situ Direct Gas Analysis of Li-ion Batteries. J. Power Sources, in press (2020).

Kalaga et al., "Insights from incorporating reference electrodes in symmetric lithium-ion cells with layered oxide or graphite electrodes", J. Power Sources 438, 227033 (2019)

Mao et al., "Evaluation of Gas Formation and Consumption Driven by Crossover Effect in High-Voltage Lithium-Ion Batteries with Ni-Rich NMC Cathodes", ACS Appl. Mater. Interfaces 11, 43235 (2019)

Morin et al. "Transition Metal Dissolution from NMC-Family Oxides: A Case Study", ACS Appl. Energy Mater. 3, 2565 (2020)

Sahore et al. "Identification of Electrolyte-Soluble Organic Cross-Talk Species in a Lithium-Ion Battery via a Two-Compartment Cell", Chem. Mater. 31, 2884 (2019)

Sahore et al. "Revisiting the mechanism behind transition-metal dissolution from delithiated $\text{LiNi}_x\text{Mn}_y\text{Co}_z\text{O}_2$ (NMC) cathodes", J. Electrochem. Soc. 167, 200513 (2020)

Shkrob et al., "Facile in Situ Syntheses of Cathode Protective Electrolyte Additives for High Energy Density Li-Ion Cells", Chemistry of Materials 31, 2459 (2019)

Tornheim et al., "Ligand-Dependent Electrochemical Activity for Mn^{2+} in Lithium-Ion Electrolyte Solutions", J. Electrochem. Soc. 166, A2264 (2019)

Tornheim et al., "Effect of electrolyte composition on rock salt surface degradation in NMC cathodes during high-voltage potentiostatic holds", Nano Energy 55, 216 (2019)

Yang et al., "4-(Trimethylsilyl) Morpholine as a Multifunctional Electrolyte Additive in High Voltage Lithium Ion Batteries", J. Electrochem. Soc. 167, 070533 (2020)

Yang et al., "Structural underpinnings of cathode protection by in situ generated lithium oxyfluorophosphates", J. Power Sources 438, 227039 (2019)